Volume 1 | Number 9 | November 2017 | Pages 1849–2030

Sustainable Energy & Fuels

Interdisciplinary research for the development of sustainable energy technologies

rsc.li/sustainable-energy

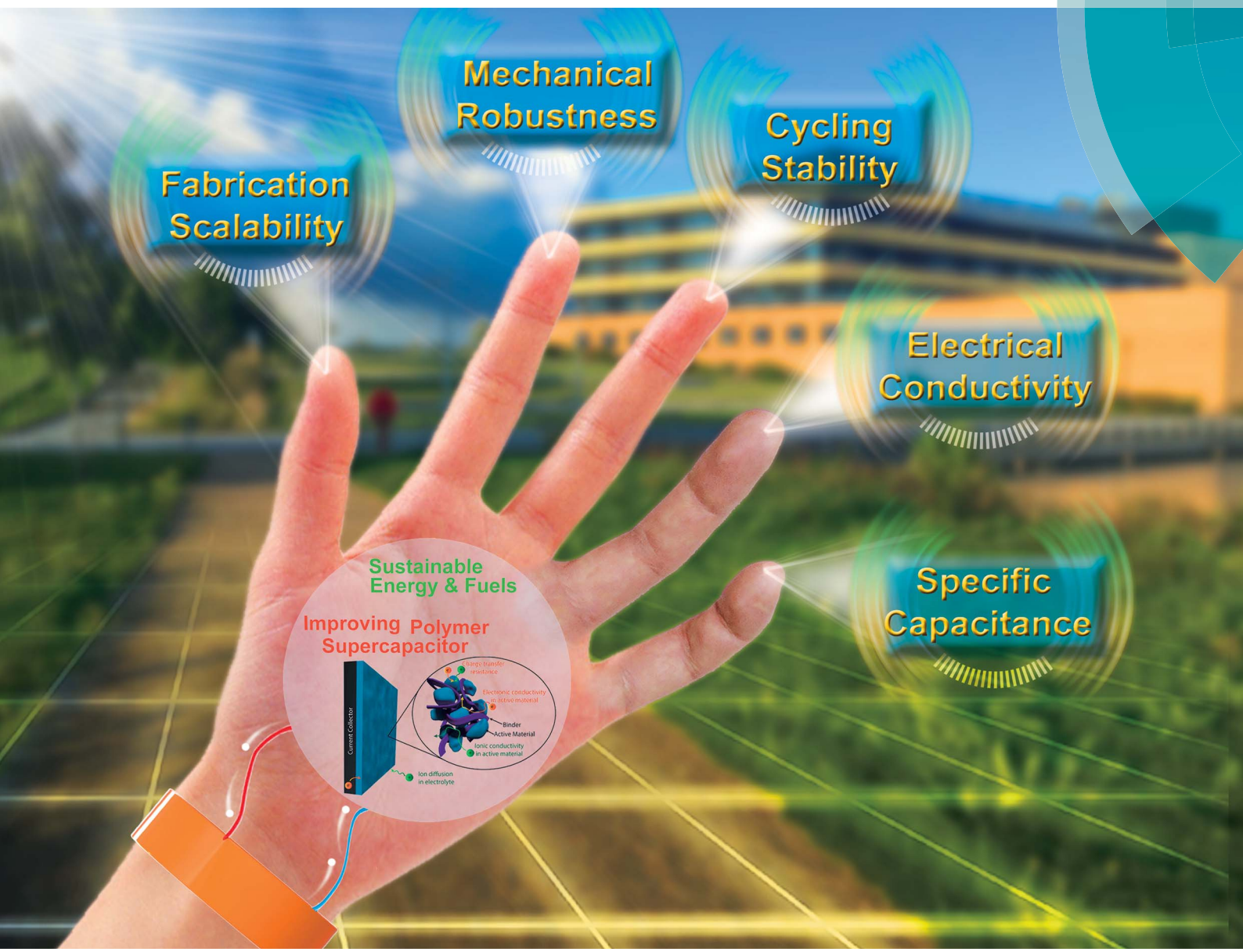

ISSN 2398-4902

ROYAL SOCIETY OF CHEMISTRY

REVIEW ARTICLE

Stoyan K. Smoukov *et al.*

Multidimensional performance optimization of conducting polymer-based supercapacitor electrodes

Sustainable Energy & Fuels

REVIEW

View Article Online
View Journal | View Issue

Cite this: *Sustainable Energy Fuels*, 2017, **1**, 1857

Multidimensional performance optimization of conducting polymer-based supercapacitor electrodes

Kara D. Fong, [a] Tiesheng Wang [ab] and Stoyan K. Smoukov*[acd]

Supercapacitors based on conducting polymers promise to bridge the gap between the high power densities of carbon-based double-layer capacitors and the high energy densities of batteries. While much work has focused on improving the specific capacitance of these materials, emerging applications also demand competitive performance with regards to a variety of other criteria, including long-term cycling stability, mechanical robustness, and scalability of fabrication. There is no consolidated summary in the literature, however, of the specific strategies used to target these individual metrics as well as the tradeoffs that exist between them. Herein, we review the most recent progress in engineering high performance conducting polymer-based supercapacitor electrodes, emphasizing the successful techniques for polymer synthesis, nanostructuring, and compositing with carbon or metal oxides which have been used to optimize each of the most important supercapacitor performance metrics.

Received 17th July 2017
Accepted 14th August 2017

DOI: 10.1039/c7se00339k

rsc.li/sustainable-energy

[a]*Department of Materials Science and Metallurgy, University of Cambridge, 27 Charles Babbage Rd., Cambridge CB3 0FS, UK. E-mail: s.smoukov@qmul.ac.uk; sks46@cam.ac.uk*

[b]*EPSRC Centre for Doctoral Training in Sensor Technologies and Applications, University of Cambridge, Philippa Fawcett Drive, Cambridge CB3 0AS, UK*

[c]*Active and Intelligent Materials Lab, School of Engineering and Materials Science, Queen Mary University of London, Mile End Road, London E1 4NS, UK*

[d]*Department of Chemical and Pharmaceutical Engineering, Faculty of Chemistry and Pharmacy, Sofia University, 1 James Bourchier Ave., 1164 Sofia, Bulgaria*

1 Introduction

Concerns over climate change and the availability of fossil fuels are driving efforts towards renewable and sustainable energy production. Although the use of these energy resources has grown significantly in recent years,[1–3] further adoption of renewables will require the development of improved energy storage technologies to regulate and distribute power generated by intermittent sources such as wind and solar.[4–6] While

Kara Fong received her B.S. with Honors in Chemical Engineering from Stanford University. She is currently pursuing an MPhil in Materials Science and Metallurgy from the University of Cambridge with the support of a Churchill Scholarship. Her work under the supervision of Dr Stoyan K. Smoukov focuses on developing polymer-based nanostructures for energy storage.

Tiesheng Wang received his BEng in Materials Science and Engineering from Imperial College London and MRes in Sensor Technologies and Applications from the University of Cambridge. Tiesheng is currently a PhD candidate and China Scholarship Council (CSC) scholarship holder in the Department of Materials Science and Metallurgy at the University of Cambridge, supervised by Dr Stoyan K. Smoukov. He is also affiliated with the Engineering and Physical Sciences Research Council (EPSRC) Centre for Doctoral Training in Sensor Technologies and Applications. Tiesheng is developing materials under nano-confinement and multifunctional materials with interpenetrating structures that can benefit sensing, energy storage, and catalysis.

batteries are currently at the forefront of energy storage today, they are inherently limited in their power density: they store energy through chemical changes and reorganization of their bulk structure, a process which presents severe kinetic limitations.[7–9] These charge storage processes also limit the lifetime of batteries, making them unsuitable for applications requiring many charge/discharge cycles.[10,11] Supercapacitors present a promising alternative to meet the current demand for improved energy storage technologies. These devices' high power density, long cycle life, low maintenance requirements, and safety make them attractive as replacements or complements to conventional lithium ion batteries.[12,13] In fact, supercapacitors are already employed on a commercial level in a variety of applications, from industrial power management to transportation and consumer electronics.[14–20]

The most thoroughly-studied form of supercapacitor is the electrochemical double-layer capacitor (EDLC). These devices store charge in the electrochemical double layer at the electrode–electrolyte interface: when solvated ions from the electrolyte electrostatically adsorb onto a charged electrode, the resulting charge separation produces double-layer capacitance.[21,22] The simplest model of this process (the Helmholtz model) describes double-layer capacitance using the equation for a parallel plate capacitor:[23]

$$C = \frac{\varepsilon A}{d}$$

where C is the double-layer capacitance, ε is the permittivity of the dielectric separating the charges, A is the surface area of the electrode, and d is the distance between the electrode and electrolyte ions. EDLCs are typically made from carbon-based materials, which can be synthesized with extremely high surface areas (typically up to 1000–2000 $m^2\ g^{-1}$)[24] and possess the additional advantages of high conductivity, low cost, and well-established processing techniques.[24–28] These carbon-based EDLCs typically exhibit specific capacitance values ranging from 50 F g^{-1} to 350 F g^{-1}.[16,29,30]

In addition to the non-faradaic double-layer charge storage process utilized in EDLCs, other classes of materials store charge through pseudocapacitance: fast, reversible redox reactions at or near the electrode surface, including ion intercalation, underpotential deposition, or specific adsorption of ions.[31,32] These additional charge storage mechanisms allow for increased capacitance and have the potential to bring the energy density of supercapacitors closer to that of batteries while maintaining the high power density of EDLCs.

Of these pseudocapacitive materials, conducting polymers show particular promise for high-performing supercapacitor devices. First demonstrated for supercapacitor applications in the 1990s,[33] conducting polymers exhibit pseudocapacitance through doping and de-doping of the polymer backbone, which results in intercalation and de-intercalation of electrolyte ions within the polymer electrode to maintain charge neutrality.[34] This charge storage mechanism allows many conducting polymers, namely polyaniline (PANI), poly(3,4-ethylenedioxythiophene) (PEDOT), and polypyrrole (PPy), to exhibit specific capacitance comparable to or higher than many metal oxides, the other main class of pseudocapacitive material.[30,35] Conducting polymers are also advantageous based on their high conductivity (imparted by their conjugated backbones, which allow for delocalization of π-electrons over the entirety of the polymer chain),[36–38] low cost, and facile processability.[39,40] Furthermore, their mechanical properties have the potential to enable supercapacitors which are lightweight, stretchable, or flexible, key drivers for integration into novel technologies such as wearable electronics, roll-up displays, or bio-implantable devices.[41–43] These advantages over other

Stoyan Smoukov is a Senior Lecturer at Queen Mary University of London. He has also been the Head of the Active and Intelligent Materials group at the University of Cambridge since 2012. He has co-founded a startup company for producing nanofibers, and published 70 journal papers, cited over 1850 times, with H-index of 20. Research interests include artificial morphogenesis, fundamentals of confinement, and combining geometry and chemistry to achieve multi-responsive materials. Longer term goals include incorporating movement, sensing, and power sources to create autonomous material robotics.

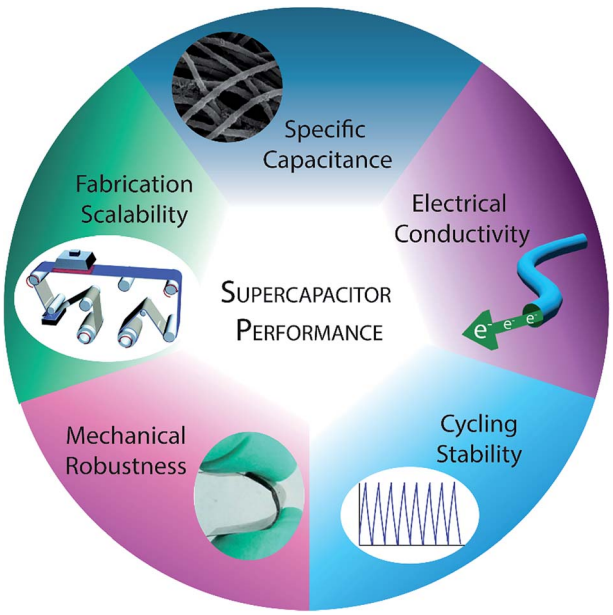

Fig. 1 Summary of the main criteria for successful supercapacitor performance. Specific capacitance icon adapted with permission from ref. 44. Copyright 2013 American Chemical Society. Mechanical robustness icon adapted with permission from Macmillan Publishers Ltd: Scientific Reports,[45] copyright 2013. Fabrication scalability icon adapted from ref. 46 with permission from The Royal Society of Chemistry.

classes of supercapacitor material have motivated much research effort towards developing enhanced conducting polymer-based electrodes.

Here, we review the recent progress in optimizing several of the most crucial performance metrics for conducting polymer-based supercapacitors (Fig. 1): specific capacitance, electrical conductivity, cycling stability, mechanical robustness, and fabrication scalability. An understanding of the synthesis and nanostructuring techniques available to specifically influence each of these individual performance criteria will be crucial for the rational design of improved conducting polymer electrodes.

2 Specific capacitance

2.1 Charge storage fundamentals

A supercapacitor electrode's capacitance – its ability to store electric charge – provides the most direct insight into its energy storage capabilities, as energy scales linearly with capacitance:

$$E = \tfrac{1}{2}CV^2$$

where E is energy (J), C is capacitance (F), and V is voltage (V). Most commonly, capacitance is normalized based on the mass of active material in the electrode (yielding specific capacitance), although areal or volumetric capacitance may be more appropriate for some applications.[47]

A supercapacitor's capacitance is affected foremost by the chemical identity and charge storage mechanism of the active material. For conducting polymers, maximum values of theoretical specific capacitance (C_{Th}, F g^{-1}) are dictated by the polymer's doping mechanism and available oxidation states and can be calculated using the following equation:[48]

$$C_{Th} = \frac{\alpha \times F}{\Delta E \times M}$$

where α is the doping level per monomer unit, F is the Faraday constant (C mol^{-1}), ΔE is the operating voltage range (V), and M is the molecular weight of the monomer (g mol^{-1}). Values of C_{Th} for common conducting polymers are listed in Table 1. Based on theoretical specific capacitance alone, PANI serves as the most competitive option for high performance conducting polymer supercapacitors. As described in the following sections, however, additional considerations must be made when selecting the optimal material for practical applications.

Note that these theoretical capacitance values can vary from source to source depending on the assumptions used in the above calculation. The doping levels (α) in Table 1 serve as representative average levels under standard conditions but in practice can vary significantly depending on the identity of the dopant and processing methods used. PPy, for example, has been shown to exhibit doping levels ranging from 20–40%.[49] One must also consider the reversibility of the doping process when reporting the value of α. The value of 0.5 for PANI in Table 1 assumes a fully reversible process of doping from the leucoemeraldine to the emeraldine state.[50] Some sources perform this calculation assuming an α value of 1, corresponding to the transition to the fully oxidized pernigraniline state. This higher doping level, however, induces irreversible chemical changes to the polymer, making the resulting higher C_{Th} value impractical for real world applications.[48] The values of ΔE in the above equation can vary between sources as well based on the assumed doping level (a higher doping level for a given polymer will require a greater voltage window) and the testing conditions used, such as the identity and concentration of the electrolyte ions.[51] Furthermore, the theoretical capacitance calculation described here ignores the contribution of double-layer charging, which will occur in parallel to pseudocapacitive doping and increase the overall capacitance of the device. This contribution will be proportional to the surface area of the

Table 1 Theoretical capacitance and properties of three of the most common conducting polymers. Adapted from ref. 53, Copyright 2004, with permission from Elsevier

Polymer	M (g mol^{-1})	α	ΔE (V)	C_{Th} (F g^{-1})
PANI	93	0.50	0.7	750
PPy	67	0.33	0.8	620
PEDOT	142	0.33	1.2	210

electrode and is often assumed to have a maximum value of 320 F g^{-1} by analogy with high surface area activated carbon.[48,52]

Capacitance values far above the aforementioned theoretical limits can be achieved by forming composite structures with carbon and/or metal oxides. Carbon-based composites typically enhance the surface area of an electrode, increasing the contribution of double-layer capacitance,[54–56] while composites with metal oxides introduce additional charge storage mechanisms to the system.[57] Furthermore, as discussed in the following sections, compositing can also improve the material utilization efficiency, conductivity, or cycling stability of an electrode. Experimental capacitance values for various conducting polymers and polymer-based composites are summarized in Fig. 2.

In both composite and pure-polymer systems, the specific capacitance is often much lower than the theoretical limits. This discrepancy can in large part be attributed to inefficient utilization of the active material: due to the relatively low ionic conductivity and often dense structure of conductive polymer films, typical pseudocapacitive processes only take place within the first few tens of nanometers of the electrode–electrolyte interface (Fig. 3a).[16,58] Consequently, any active material deeper within the bulk of the electrode is wasted, decreasing the specific capacitance of the electrode. This issue is particularly pronounced at high charge/discharge rates, where the slow kinetics of ion diffusion can impact device performance even more drastically.

Strategies for improving both the specific capacitance and rate capability of conducting polymer electrodes are thus largely focused on increasing material utilization efficiency: creating high surface area nanostructures which possess short ion diffusion length scales and allow facile infiltration of electrolyte throughout the electrode bulk (Fig. 3b).

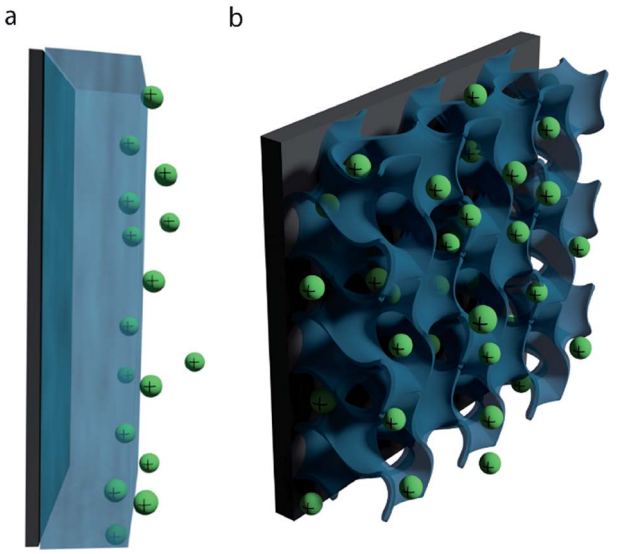

Fig. 3 Material utilization efficiency in bulk and nanostructured electrodes. (a) Illustration of a bulk polymer film, in which low ionic conductivity prevents active material in the bulk from participating in pseudocapacitive reactions. (b) A nanostructured electrode with high surface area, short ion diffusion distances, and facile electrolyte infiltration properties for enhanced specific capacitance.

2.2 Enhancing material utilization efficiency

Efficient material utilization requires the majority of the pseudocapacitive material to be located within nanometers of the electrode–electrolyte interface. It should be noted that simply utilizing very thin films of active material can eliminate issues with ion diffusion kinetics and nominally circumvent this issue. Zhang *et al.* fabricated an ultrathin (300 nm) layer of PEDOT:PSS on graphite foil which maintained its capacitive performance even at ultrahigh scan rates up to 1000 V s^{-1}.[59] Although these electrodes were suitable for the AC line-filtering for which they were designed, however, most practical applications require a much larger total mass or volume of active material. Moreover, the small masses utilized for thin, flat films often introduce experimental error.[53] One of the primary challenges for optimal ion mobility is therefore to develop nanostructuring techniques which yield short diffusion lengths within bulk materials without sacrificing the total quantities of active mass necessary for sufficient energy storage.

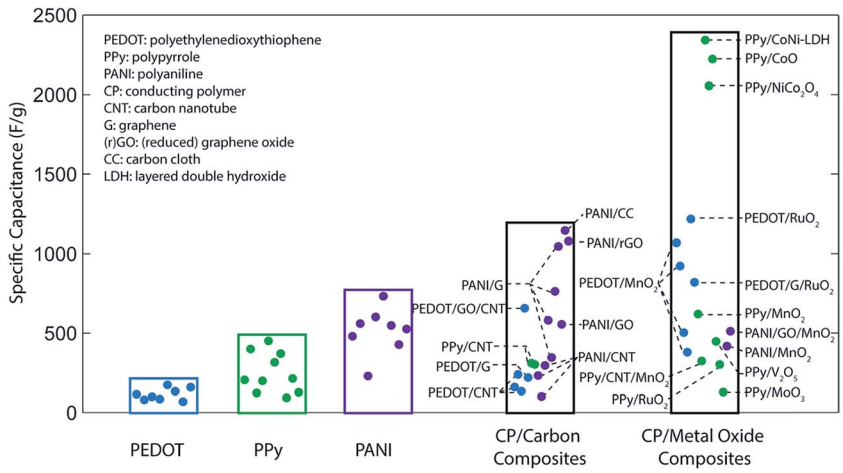

Fig. 2 Comparison of the specific capacitance of conducting polymer-based supercapacitors.

One-dimensional (1D) materials are particularly attractive for this purpose due to their high surface area and high aspect ratios. Polymer-based filamentous structures (nanowires,[60–62] nanorods,[63–65] and nanofibers[44,66,67]) (Fig. 4a), synthesized by techniques such as templating, electrospinning, or lithography,[68] have all been utilized in high-performing electrodes. The ordering of these 1D materials plays a significant role in determining material utilization efficiency: vertically-aligned PANI nanowire arrays on graphene oxide sheets have been shown to achieve a specific capacitance of 555 F g^{-1} (Fig. 4b), whereas randomly-oriented PANI nanowires fabricated by the same method yielded only 298 F g^{-1}.[69] In the former case, the regular ordering of the arrays maximized the overall quantity of PANI in the supercapacitor which was accessible to the electrolyte and thus able to participate in pseudocapacitance reactions. To further optimize 1D morphologies like this, it can be useful to estimate the average diffusion length of ions in the electrode. This can be accomplished using a known diffusion coefficient for the given polymer/electrolyte system[70] and a characteristic diffusion time, determined at a certain voltage using electrochemical impedance analysis. If this diffusion length is greater or equal to the diameter of the 1D polymer structure, then it can be inferred that the system is not limited by ion diffusion within the polymer.[58]

In addition to short ion diffusion distances within the active material, a high-performing conducting polymer nanostructure must also be optimized for electrolyte infiltration. Three-dimensional, high surface area morphologies are very effective for this purpose. Most commonly, conducting polymers are deposited on substrates such as nickel foam which possess uniform macroporous structures to simultaneously facilitate high surface area and facile ion diffusion.[75–77] Zhou *et al.*, for example, achieved an impressive specific capacitance of 2223 F g^{-1} using a CoO@PPy nanowire array deposited onto

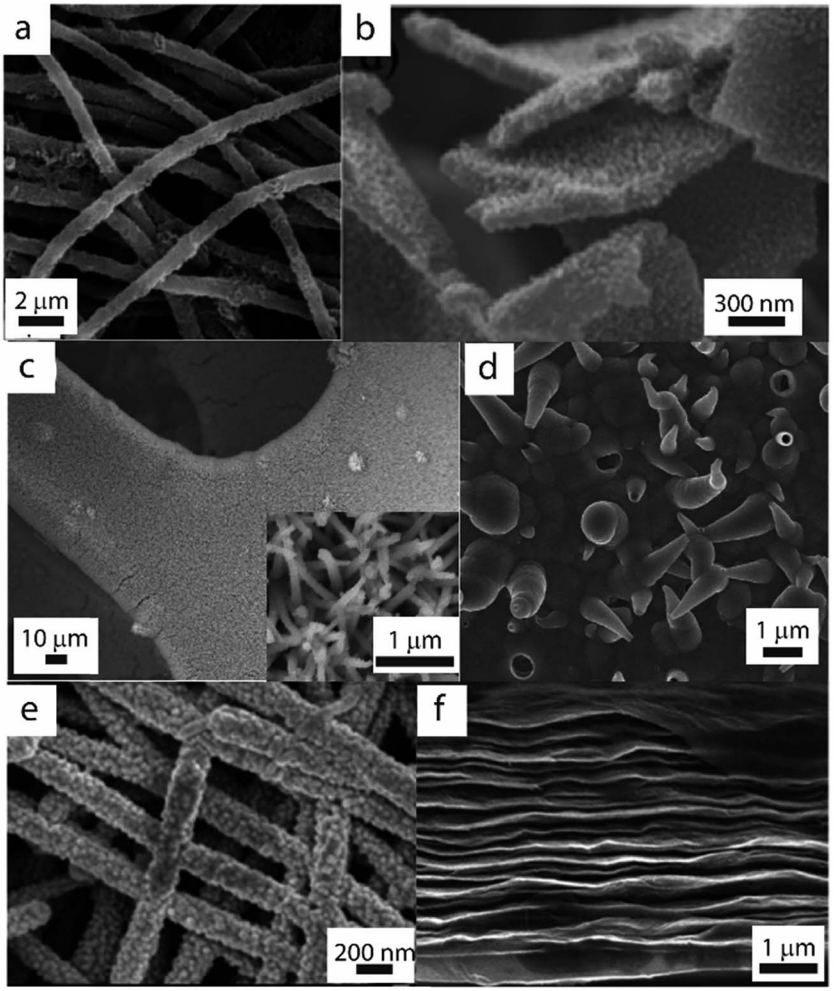

Fig. 4 SEM images of nanostructured polymer-based electrodes designed for enhanced specific capacitance. (a) Hollow PANI nanofibers formed by electrospinning. Reproduced with permission from ref. 44. Copyright 2013 American Chemical Society. (b) Vertically-aligned PANI nanowire arrays on graphene oxide sheets. Reproduced with permission from ref. 69. Copyright 2010 American Chemical Society. (c) CoO@PPy nanowires on nickel foam. Adapted with permission from ref. 71. Copyright 2013 American Chemical Society. (d) PPy film decorated with micro/nanoscale "horns". Reproduced from ref. 72, Copyright 2011, with permission from Elsevier. (e) PANI–carbon nanofiber composite paper. Reproduced from ref. 73 with permission from The Royal Society of Chemistry. (f) Layers of graphene oxide separated by PEDOT:PSS and CNTs. Reproduced from ref. 74. Copyright 2015 American Chemical Society.

nickel foam (Fig. 4c).[71] Hydrogels with large, interconnected pores have also shown promise as materials for rapid ion diffusion kinetics and excellent rate capability.[78–81] PANI hydrogels synthesized by Pan *et al.*, for example, experienced only a 7% capacitance loss upon increasing current density from 0.5 A g^{-1} to 5 A g^{-1} (from 450 F g^{-1} to 420 F g^{-1}).[82] Other surface features can drastically enhance electrolyte infiltration as well: hollow micro/nanoscale "horns" made from electropolymerization of PPy can both increase the surface area of the electrode and create pathways for transport of electrolyte to the electrode bulk (Fig. 4d).[72] These favorable traits yielded competitive rate capability, with 90% capacitance retention when increasing current density from 3 A g^{-1} to 24 A g^{-1}.

The specific capacitance and rate capability of conducting polymer-based electrodes can also be enhanced by incorporating carbon-based frameworks which decrease the packing density of the electrode materials to enhance ion mobility. These carbon structures include carbon nanotube or nanofiber networks (Fig. 4e)[53,73,83] and layers of graphene oxide sheets.[74] Islam *et al.* have demonstrated this approach by creating self-assembled layers of graphene oxide separated by PEDOT:PSS and CNTs (Fig. 4f).[74] The interlayer *d*-spacing between these sheets (300 to 650 pm) was measured to be on the order of the hydrated ionic radii of the SO_4^{2-} and H_3O^+ electrolyte ions, which facilitated effective ion penetration into the structure. The authors subsequently reported a specific capacitance of 266 F g^{-1} at a high current density of 10 A g^{-1}, a relatively small decrease compared to the value of 328 F g^{-1} at 1 A g^{-1}. This strategy of decreasing the packing density of active materials can also be carried out on a molecular level by introducing large dopants into the polymer matrix, which can create space between polymer chains enhance ionic conductivity.[84] Ingram *et al.* utilized large polysulfonated aromatic anions as a PPy dopant, which remained immobile in the polymer matrix to create bridges between the positively-charged polymer chains, thereby opening channels within the structure to facilitate ion transport.[85] These electrodes, which achieved areal capacitances of up to 0.40 F cm^{-2}, maintained good capacitive behavior at scan rates as high as 300 mV s^{-1}.

While facile electrolyte infiltration is crucial to efficient material utilization, excess electrolyte stored in porous structures can actually lower specific capacitance by introducing inactive mass to the electrode. Although increasing porosity will increase overall surface area, not all pore sizes contribute to increased capacitance: micropores (<2 nm) will typically be too small for electrolyte ions to access, and macropores (>50 nm) primarily contain redundant electrolyte, introducing wasted volume.[86] Recent work has modified the pore size distributions of conducting polymer electrodes to explore and address this issue.[87] Wang *et al.*[88] utilized quaternary amine groups to modify nanocellulose fiber substrates prior to PPy polymerization; this cationic surface modification was found to reduce the macropore volume of the polymer while maintaining the micro- and mesopore structure. The resulting pore structure was found to yield higher volumetric capacitances than PPy synthesized on unmodified substrates. While pore size optimization such as this has been heavily investigated for carbon-based EDLCs,[89–91] there are few analogous studies for pseudocapacitive materials such as conducting polymers.

Another promising means of improving ion accessibility and material utilization is the development of self-doping polymer structures.[92,93] Christinelli *et al.* developed layer-by-layer electrodes of poly(*o*-methoxyaniline) (POMA) and poly(3-thiophene acetic acid) (PTTA), in which the POMA served as the pseudocapacitive polymer and the PTTA provided carboxylate anions to balance the positive charges on the POMA.[94] This strategy reduces the need for intercalation of electrolyte ions and thus enables increased mass loading without sacrificing material utilization: the specific capacitance of these electrodes increased nearly linearly as the number of POMA/PTTA bilayers increased (up to 140 F g^{-1} for 112 bilayers).

3 Electrical conductivity

High electrical conductivity is a crucial requirement for supercapacitors, as it enables the fast charge transfer kinetics required for operating at high power. The combined effect of all the electronic and ionic resistances in a device which limit its power density are expressed as the equivalent series resistance (ESR). These sources of resistance, summarized in Fig. 5, include ion transport in the electrolyte, ion transport within the electrode, and electrical conduction within the electrode and all other device components (current collector, leads, *etc.*).[86] Much like the issues with ionic transport discussed in the previous section, enhancing electrical conductivity in supercapacitor electrodes is inherently linked with improving specific capacitance. However, given the distinct synthesis and engineering strategies which can be employed to target electrical conductivity specifically, here we discuss this as a separate performance metric for optimization of conducting polymer-based electrodes.

The electrical conductivity of a conducting polymer is largely determined by its doping level, as dopants introduce the free charge carriers responsible for the polymers' conductivity.[95] These doping levels are intrinsically limited by the structure of the conducting polymer itself based on how closely charges can

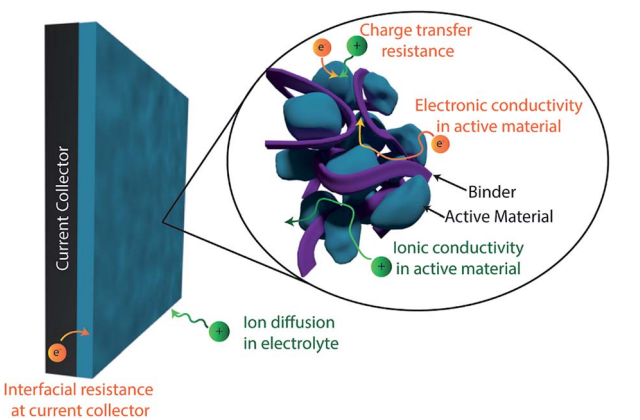

Fig. 5 Sources of electronic and ionic resistance in supercapacitor electrodes.

be spaced along the polymer chain (typically less than one dopant per monomer).[33] However, the identity of the dopant and synthesis conditions can play a large role in determining doping level. Large dopant counterions, for example, will suffer from poor mobility within the polymer during synthesis, which may lead to reduced doping levels.[96]

High electrical conductivity also requires high charge carrier mobility, both within and between polymer chains.[97–99] Intrachain conductivity is primarily limited by conjugation length and can be enhanced by minimizing the number of defects in the polymer which disrupt the delocalized π system. Inter-chain conductivity is facilitated by chain alignment and polymer crystallinity.[100–103] Growth of single crystal PEDOT nanowires through vapor phase polymerization, for example, has yielded ultrahigh conductivity of approximately 8000 S cm^{-1}; this value is higher than any reached for PANI or PPy to date.[97] The interchain π–π stacking that promotes high molecular ordering can also be enhanced using aromatic dopants, which promote anisotropic growth of polymer films and thus higher conductivity compared to films grown with spherical, non-aromatic dopants.[96] Interfacing conducting polymers with graphene is also an effective strategy for enhancing crystallinity, as the strong π–π interactions introduced by graphene promote compact packing and high inter-chain charge carrier mobility.[104,105] Kim *et al.* demonstrated the use of a PANI/reduced graphene oxide (rGO) film which achieved a conductivity of 906 S cm^{-1}, higher than that of PANI or the rGO alone (580 S cm^{-1} and 46.5 S cm^{-1}, respectively).[106]

In addition to the resistance originating within the polymer itself, further sources of resistance may arise when integrating conducting polymers into electrodes. It is common practice to use nonconductive polymer binders such as polytetrafluoroethylene and polyvinylidene fluoride (PVDF) to adhere the electrode material to the current collector.[107–109] These insulating binders limit the electrode's electronic conductivity, often reduce ionic conductivity (due to their hydrophobicity), and reduce specific capacitance by adding inactive weight to the electrode.[110] Some effort has been devoted to developing binder materials made from conducting polymers, including PEDOT/graphene oxide composites[110,111] or PANI combined with additives such as aromatic sulfonic acid dopants and polyol.[112] The latter approach by Kang *et al.* yielded binders with 20–25% greater adhesion than the conventional PVDF, with an electrical conductivity of 1.1 S cm^{-1}.[112]

Interfacial resistance between the active material and current collector can also impact a device's ESR. Certain anionic dopants can address this issue by increasing adhesion of the polymer active material to the substrate. Dopants with chelating properties such as tiron (a sulfonate aromatic compound)[113,114] and sulfanilic acid azochromotrop[115] have been reported to promote uniform and adherent film formation: their phenolic hydroxyl groups are able to deprotonate and bind with the metal ions of the current collector, which both improves polymer adhesion and facilitates charge transfer.[113]

Most commonly, these issues with binders and current collector adhesion are addressed by synthesizing the electrode's active material directly onto the currently collector or fabricating the active material as a freestanding film.[116] The former strategy is commonly accomplished by synthesis (typically electrochemical polymerization) directly onto high surface area conductive substrates such as nickel foam,[75–77,117] carbon nanotube-based frameworks,[118,119] or graphene.[104,120]

Note that while improvements to the conductivity of conducting polymer-based electrodes such as these are certainly beneficial, electrical conductivity is less of an issue for conducting polymers than it is for other classes of supercapacitor material. In fact, many have used conducting polymers as a means of improving the conductivity of other materials.[119,121,122] This approach is most common for MnO_2-based supercapacitors, as the primary limitation of MnO_2 is its poor conductivity (10^{-5} to 10^{-6} S cm^{-1}).[123–126] While several groups have improved the conductivity of MnO_2-based electrodes by creating carbon composites,[127–132] many efforts to use conducting polymers for this purpose have also been quite successful.[133–135] Yu *et al.*,[136] for example, employed PEDOT:PSS as a "conductive wrapping" for graphene/MnO_2 electrodes. The additional electron transport paths provided by the polymer coating not only decreased the electrode's equivalent series resistance from 87 Ω to 27 Ω, but it also increased the specific capacitance by 45%, to 380 F g^{-1}.[136] Similarly, conductive polymers have been used to enhance the conductivity of electrodes based on V_2O_5 (ref. 137) and $NiCo_2O_4$.[138]

Conductive polymers have also been used to impart conductivity on metal–organic frameworks (MOFs);[139,140] these materials have the potential to be very effective for supercapacitors based on their well-defined porous structure,[141,142] which creates a high surface area and enables facile ion transport. However, most MOFs are not conductive, making it difficult to take advantage of this promising structure. Wang *et al.* demonstrated electrochemical deposition of PANI onto a cobalt-based MOF, yielding a conductive, high-surface area electrode with a specific capacitance of 371 F g^{-1} (2146 mF cm^{-2}).[139]

4 Cycling stability

4.1 Swelling-induced degradation

Long-term cycling stability is one of the primary challenges in conducting polymer supercapacitors. In contrast to EDLCs, which can maintain stable capacitance values for over 100 000 cycles,[26,143] many conducting polymer electrodes retain less than 50% of their original capacitance values after only 1000 cycles.[77,144–146] These long-term stability issues are largely caused by mechanical fatigue induced by the volumetric changes that takes place during cycling. As the polymer is oxidized or reduced during charging/discharging, ions from the electrolyte intercalate in or out of the material to maintain charge neutrality, which causes the active material to swell or shrink.[147,148] This process can damage the microscopic hierarchical structure of the electrode as well as cause molecular-scale disruptions such as polymer chain disorder or the collapse of ion flow channels, rendering the polymer unable to effectively store charge.[49,149]

One of the dominant approaches for improving supercapacitor stability is to incorporate conducting polymers into

open and/or flexible networks which can adapt to volumetric changes and thus maintain the mechanical integrity of the electrode after repeated cycling. Carbon-based composites are well-suited for this purpose. CNTs, for example, can be fabricated into open networks, resulting in electrodes with free space that allows for conducting polymer swelling/shrinking.[150–154] Chen *et al.* demonstrated this approach by electrodepositing PPy onto CNT films, achieving 95% capacitance retention after 10 000 cycles.[154] Layers of graphene or graphene oxide sheets can also serve as open frameworks to accommodate volumetric changes.[155–157] PANI nanolayers synthesized between graphene sheets retained 85% of their capacitance after 60 000 cycles, as the space between the sheets provided room for expansion of the polymer without damage to the overall hierarchical structure.[157] Stability enhancements can be achieved through a similar mechanism by compositing conducting polymers with MXenes. Layering PPy between 2D layers of titanium carbide yielded electrodes with almost no capacitance degradation after 20 000 cycles, while pristine PPy retained only 70% of its capacitance under the same conditions.[158] As was the case for layered graphene sheets, the titanium carbide sheets accommodated the swelling of the conducting polymer; this process is facilitated by the strong chemical interactions between the polymer and MXene.[158,159]

Volumetric changes during charging/discharging can also be accommodated using composites based on polymers alone. The flexible, porous nature of hydrogels makes these structures particularly effective in alleviating mechanical stress during cycling:[160–162] polyaniline-containing hybrid hydrogel networks have achieved 92% capacitance retention after 35 000 cycles.[149] Recent work in developing interpenetrating networks of conducting polymer in a flexible, cross-linked ionically conductive matrix has also yielded enhancements in cycling stability: PEDOT interpenetrated in a PEO-based network yielded 97.5% capacitance retention after 3000 cycles, while neat PEDOT prepared under similar conditions retained only 82% after 1200 cycles[163] (Fig. 6a). In this structure, the flexible PEO network served as a mechanical buffer to suppress mechanical stress in the electrode.

Cycling stability can also be improved by introducing a protecting layer to suppress the polymer's volumetric changes. Adding a thin carbonaceous shell to PANI or PPy nanowires has been shown to drastically improve cycling stability. For the case of carbon-coated PPy, 85% capacitance retention was observed after 10 000 cycles, while bare PPy tested under the same conditions retained less than 25% of its initial capacitance after 10 000 cycles (Fig. 6b).[145] This approach has been utilized for other materials as well: in one case, the addition of a thin carbonaceous layer on polyvinylferrocene/polypyrrole hybrids enabled capacitance retention of 94.5% after 3000 cycles (without the coating, only 60% retention was observed after 1000 cycles).[165] More recently, PANI nanowires have been confined inside 10 nm-diameter CNTs to achieve a similar effect in which the CNT nano-channels help suppress structural changes of the polymer throughout cycling.[166] It should be noted however, that the addition of a carbon protecting layer can negatively impact the electrode's rate capability, as the carbon hinders ion diffusion to the polymer core.[145] Tradeoffs such as this between stability and rate capability must be taken into consideration when designing an electrode for a particular application.

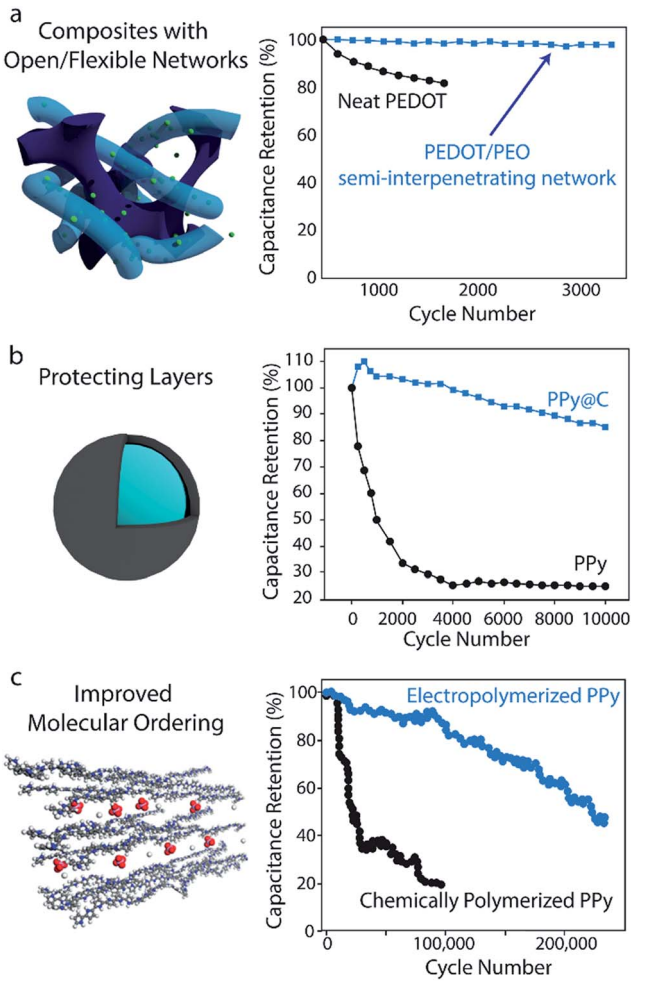

Fig. 6 Strategies for enhancing polymer-based supercapacitor cycling stability. (a) Composites with open/flexible networks. Data shows the stability improvements upon interpenetrating PEDOT in a flexible, ionically conducting PEO network. Adapted with permission from ref. 163. Copyright 2017, American Chemical Society. (b) Protecting layers. The stability enhancements imparted by introducing a carbon protecting layer over PPy electrodes is shown. Graph is adapted with permission from ref. 145. Copyright 2014, American Chemical Society. (c) Improved molecular ordering. Data shows the results of improving the molecular ordering of PPy through electropolymerization. Schematic and data are adapted with permission from ref. 164. Copyright 2016, American Chemical Society.

Metal oxides have also been successfully used as protecting layers for conducting polymers, which has the added benefit of introducing additional charge storage mechanisms to generally increase specific capacitance. Xia *et al.* demonstrated RuO_2 to be an effective protecting layer by synthesizing core–shell PANI–RuO_2 nanofiber arrays.[167] They attribute the material's high stability (88% capacitance retention after 10 000 cycles) to the metal oxide's ability to tolerate the polymer's volumetric changes and prevent structural changes to the PANI nanofiber

during cycling. Moreover, as RuO_2 itself is a highly pseudocapacitive material, the addition of the protecting layer enabled a high specific capacitance of 710 F g^{-1}. Note, however, that the prohibitively high cost of RuO_2 would make electrodes like this difficult to scale to a commercial level. Shao *et al.* demonstrated the promise of the protecting layer approach as well, coating PPy nanowires with layered double hydroxides based on nickel and cobalt.[168] While their pristine PPy nanowires retained only 24.7% of their specific capacitance after 2000 cycles, the NiCo core–shell structure retained 90.7% after the same number of cycles – an increase which can once again be attributed to the protecting layer suppressing the polymer's swelling and shrinking.

Synthesis strategies that improve the molecular ordering of a conducting polymer can also enhance cycling stability. Recently, Huang *et al.* demonstrated 97% specific capacitance retention after 15 000 cycles and 86% retention after 100 000 cycles for electropolymerized PPy on a stainless steel mesh (Fig. 6c).[164] These capacitance retention values are significantly higher than those of most electrodes made from pure conducting polymers. It is hypothesized that the electropolymerization process used in this work promotes good molecular ordering, which creates uniform stress distribution and fast charge transfer throughout the polymer. However, further investigations are necessary given that many conducting polymer electrodes synthesized by similar electropolymerization methods do not achieve such impressive stability.[169,170] Select anionic dopants can also influence molecular-scale ordering to improve stability as well. Doping PPy with β-naphthalene sulfonate ions has yielded electrodes with 97.5% capacitance retention after 10 000 cycles;[144] these bulky anions are largely immobile in the polymer matrix and thus prevent the collapse of ion conducting channels during cycling.

4.2 Overoxidation-induced degradation

In addition to these issues induced by volumetric changes, overoxidation of the polymer caused by operating outside of an appropriate potential window can also limit long-term device performance.[49,171] PANI, for example, will degrade at high potentials to yield products such as hydroquinone and *p*-aminophenol.[172,173] Similarly, in polythiophene-based polymers such as PEDOT, sulfur from the thiophene ring can bond to oxygen from the solvent at high potentials, ultimately resulting in the production of SO_2.[174–176] In both of these cases, irreversible chemical changes disrupt the conjugated polymer backbone, drastically decreasing the electrical conductivity (and thus the charge storage ability) of the material.[177] PPy nanobrush electrodes, for example, have exhibited 80% capacitance retention after 30 000 cycles when operated over a range of 0.6 V, but when operating at 0.8 V the electrodes reached 80% retention at only 12 000 cycles.[178]

The operating voltage of a supercapacitor can be enhanced without these overoxidation issues using an asymmetric device configuration, in which the two electrodes are composed of different polymers with distinct stable potential windows.[179] In this case, it is possible for the maximum voltage window of a device to reach the stability limit of the electrolyte (1.0–1.3 V for aqueous electrolytes and 2.5–2.7 V for organic electrolytes).[180] Capacitance retention under high voltage windows can also be enhanced using pretreatments at lower voltages. Priming PANI nanofiber electrodes by performing 10 000 cycles from 0 to 0.5 V at 25 A g^{-1} before increasing the upper voltage to 0.8 V has been shown to yield significant improvements in stability: after this pretreatment, the electrodes exhibited 93% capacitance retention after 10 000 cycles, while electrodes without the pretreatment retained only 87% of their initial capacitance under the same 0.8 V window.[181] It is hypothesized that this priming process gradually relaxes the molecular structure of the polymer to improve electrochemical stability. Given that this type of pretreatment can require several hours, however, this strategy may not be suitable for all applications.

5 Mechanical robustness

The unique mechanical properties of conducting polymers enable supercapacitor electrodes which exhibit flexibility, stretchability, or toughness while maintaining competitive energy storage properties. The mechanical stability challenges here are of a different nature than the ones caused by swelling and de-swelling by doping ions: they are affected by the shape factors of the structure and stretching/bending/shear stresses induced by macroscopic deformations.

5.1 Flexible supercapacitors

Of these desired mechanical properties, flexibility has been studied the most thoroughly in the supercapacitor field, most commonly using carbon-based electrodes.[182,183] However, the energy storage capacity of these EDLC materials is limited by their lack of pseudocapacitance. Thus, integrating conducting polymers into carbon-based substrates provides a means of achieving high flexibility without sacrificing high specific capacitance.[58,184–186] The high inherent flexibility of PPy makes it particularly popular for this application relative to PANI or PEDOT.[30] Zhou *et al.*, for example, developed solid-state supercapacitors from composites films of CNTs and PPy.[187] These devices exhibited nearly unchanged capacitive behavior upon bending to 120°, folding into an 'S' shape, and twisting (Fig. 7a). Although carbon-based composites such as these are the most common class of flexible supercapacitor electrode, the inherent flexibility of many polymers enables the fabrication of pure polymer-based flexible electrodes without carbon as well.[188–190] Shi *et al.*, for example, synthesized PPy hydrogels which exhibited less than 3% capacitance decrease when bent to a radius of curvature of 3 mm.[191] The group attributed this high flexibility to the open space created by the pores of the PPy network, which can accommodate deformations during bending. Flexible materials such as these show particular promise in applications for wearable electronics, as demonstrated by recent work to create ring-shaped supercapacitor devices[41] (Fig. 7b) or weavable supercapacitor fibers[42] out of these materials.

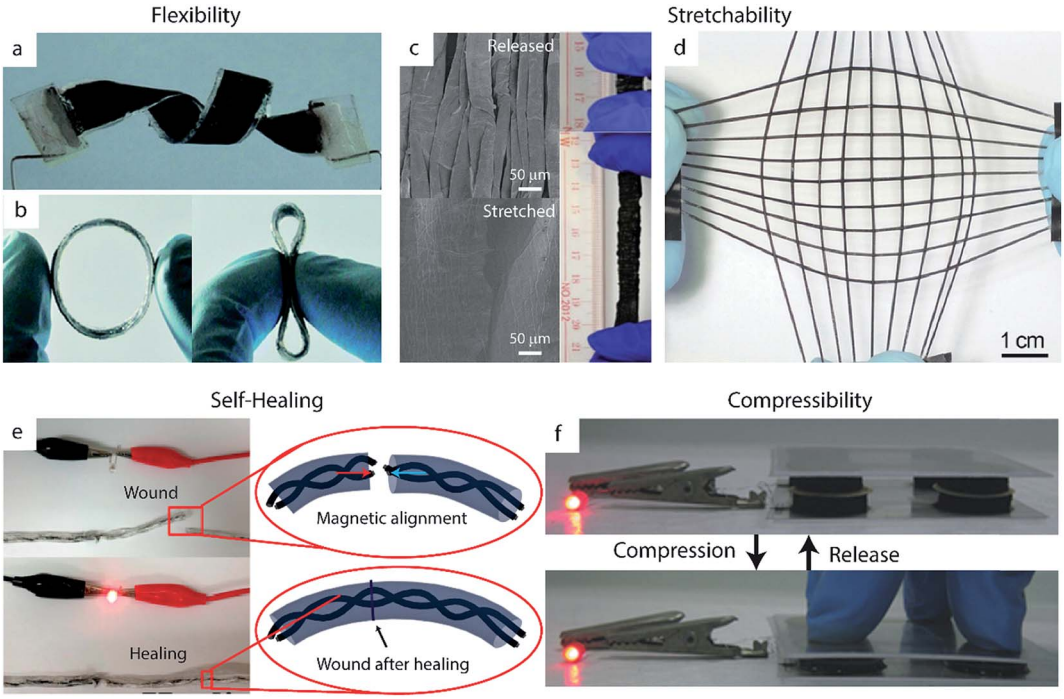

Fig. 7 Successful demonstrations of mechanical robustness in polymer-based supercapacitor devices. (a, b) Flexible devices. (a) A twisted device made from CNTs and PPy electrodes. Adapted from ref. 187 with permission from The Royal Society of Chemistry. (b) A flexible ring-type supercapacitor made from PEDOT:PSS/CNT wound onto an elastic polymer ring. Adapted from ref. 41 with permission from The Royal Society of Chemistry. (c, d) Stretchable devices. (c) SEM images of PPy/CNT paper electrodes in a relaxed state (above) and stretched state (below), with digital images (right) of the devices under 0% and 600% strain. Adapted from ref. 192 with permission from Nature Publishing Group. (d) A fiber-shaped supercapacitor made from a CNT/PANI composite deposited on pre-strained elastic polymer fibers. Reproduced with permission from ref. 193. Copyright 2014 WILEY-VCH Verlag GmbH & Co. KGaA, Weinheim. (e) A self-healing PPy-based supercapacitor on a yarn substrate, with insets showing schematic illustrations of the self-healing process. Adapted with permission from ref. 194. Copyright 2015 American Chemical Society. (f) A compressible device based on PPy/CNT sponge electrodes. Adapted with permission from ref. 195. Copyright 2015 WILEY-VCH Verlag GmbH & Co. KGaA, Weinheim.

5.2 Stretchable supercapacitors

Stretchability is another key trait for supercapacitors implemented in practical applications. Conducting polymers are particularly well-suited for this application given that they possess some inherent stretchability.[196] Thus, they can be integrated into stretchable devices without the use of complex fabrication techniques: while rigid materials such as metals are typically incorporated into stretchable electrodes using serpentine structures or percolating nanostructured films, stretchable conducting polymer electrodes can be formed simply by using highly stretchable substrates such as textiles or polymer films.[197–199] Nylon, for example, has been used as an effective substrate for PPy to create electrodes which can undergo 1000 stretching cycles under 100% strain without significant loss of specific capacitance.[200]

The stretchability of these electrodes can be enhanced further by creating wavy or buckled structures, in which the active material and/or substrate is deposited onto a pre-strained polymer and subsequently released to a relaxed state. CNT films have been particularly well-studied as wavy stretchable substrates for conducting polymer-based electrodes.[41,193] Thin films of PPy on wavy, pre-strained CNT paper, for example, can reach 600% strain without damage to the electrodes' mechanical or electrochemical properties (Fig. 7c).[192] This approach can be generalized to fiber-shaped devices as well. Zhang *et al.* wrapped CNT sheets on pre-strained elastic polymer fibers, which were then used as a substrate for PANI electrodeposition (Fig. 7d).[193] Their electrodes were able to stretch to over 400% of their original length without any significant changes in specific capacitance and maintained approximately 75% of their specific capacitance (decreasing from 106 F g^{-1} to 79 F g^{-1}) even after 5000 cycles of applying a 300% strain then relaxing. Fiber-like devices such as these can enable omnidirectional stretching when woven into textiles.[42,193] Omnidirectional or biaxial stretching can also be achieved by altering the pre-strain process of planar electrodes; such electrodes made from depositing CNT films and PANI on omnidirectionally stretched silicon rubber achieved good performance under omnidirectional strains of 200%.[201]

Note that in many instances the specific capacitance of a device increases while stretched.[41,192,200] This phenomenon can be attributed to improved conductivity upon stretching, which may be caused by greater contact between the polymer and the substrate as well as improved molecular ordering within the polymer. Stretching can increase the electrode surface area as well by expanding wrinkles which were

previously inaccessible to the electrolyte. In solid state devices, stretching can also improve the interfacial contact between the electrode and electrolyte and/or decrease the distance separating the two electrodes.[192,202,203]

5.3 Self-healing supercapacitors

Recent efforts have sought to enhance the mechanical robustness of supercapacitors even further by developing self-healing devices, an improvement which could drastically increase device lifetimes and reliability.[204,205] These devices typically employ self-healing polymers (*e.g.* carboxylated polyurethane (PU)) as substrates or coatings, which usually derive their self-healing properties based on hydrogen bond-based supramolecular interactions.[206,207] Sun *et al.*, for example, utilized self-healing polymer fibers (synthesized from the Leibler method)[208] as supports for a composite of aligned carbon nanotubes and PANI, yielding an electrode that retained 92% of its initial capacitance after breaking and healing.[209] More recently, Wang *et al.* coated graphene oxide and PPy-based fiber springs with a self-healing PU shell to achieve 52.4% capacitance retention after three healing cycles.[210]

Self-healing supercapacitors can also be fabricated using self-healing electrolytes.[211,212] In contrast to the use of self-healing substrates or coatings, this approach does not add any additional inactive weight or volume to the device (which would lower specific capacitance).[212–214] Huang *et al.* demonstrated supercapacitor devices with PPy@CNT electrodes and a self-healing, dual-crosslinked polyacrylic acid electrolyte which completely retained its capacitance after 20 healing cycles.[192]

A particular challenge in the development of self-healing devices is ensuring re-alignment of the active materials upon healing, which is crucial for restoring electrical conductivity. This misalignment issue can be addressed manually by simply applying small patches of conductive material such as CNT paper.[192] Options for autonomous re-alignment exist as well: Huang *et al.* incorporated magnetic nanoparticles into their PPy-based supercapacitors to help facilitate this process (Fig. 7e).[194] Their yarn-based supercapacitors were also coated in a self-healing polyurethane shell to further promote reconnection of broken areas. The device retained 71.8% of its initial specific capacitance after four cycles of damage/healing.

Note that the conducting polymer active material itself does not participate in the self-healing mechanism in any of the aforementioned devices. While a limited number of groups have worked towards integrating pseudocapacitive polymers into conductive, self-healing materials,[215–217] none of these polymers have been integrated into supercapacitor devices thus far. This remains a promising opportunity for next-generation self-healing supercapacitors.

5.4 Other mechanically robust supercapacitors

In addition to flexibility, stretchability, and self-healing properties, other supercapacitors have been optimized to withstand a variety of other forms of mechanical impact. Compressible electrodes, for example, can recover their initial shape after undergoing large compressive deformation.[218,219] These electrodes are formed by synthesizing conducting polymers onto compressible substrates such as hydrogels[220] or CNT sponges (Fig. 7f).[119,195] PPy–graphene foam developed by Zhao *et al.*, for example, maintained its capacitive behavior after 1000 cycles of 50% compression and relaxation due to its highly porous and flexible structure.[221] Polymer-based supercapacitors have also been engineered for resilience to cutting or tearing. Lyu *et al.* formed damage-resistant rGO/PPy composite electrodes using carbon fiber-reinforced cellulose substrates.[222] The cellulose in these electrodes provided high surface area and good intrinsic flexibility, while the carbon fibers improved the electrical conductivity and mechanical strength of the electrode – even upon damage of the cellulose fibers after repeated folding or tearing, the carbon fibers maintained the structural and electrical integrity of the substrate. Thus, the electrodes continued to perform well even after undergoing severe damage: after being cut twice the device maintained 93% of its specific capacitance, and after even more severe damage the supercapacitor exhibited 84% capacitance retention.

6 Fabrication scalability

Despite the advances made in optimizing conducting polymer-based supercapacitors, the fabrication routes for many of the most successful electrodes are either too complex or costly to be implemented commercially. While other flexible electronic technologies such as electrochromic devices,[223] organic solar cells,[224] and organic LEDs[225,226] have made great strides in integrating high-throughput roll-to-roll (R2R) fabrication techniques, the supercapacitor field has largely lagged behind in achieving similar advances. In fact, some of the most widely-used conducting polymer-based electrode fabrication techniques are severely limited in their scalability.[227] Electropolymerization, for example, cannot be integrated into R2R processing techniques and can often be time-intensive and costly.[228] Other synthesis methods such as those based on templates (*e.g.* anodic aluminum oxide, block copolymers, or porous silicate) can also be expensive and require tedious post-processing steps that limit throughput.[40,229]

One of the central requirements for integrating a synthesis method with R2R processes such as gravure coating, screen printing, or inkjet printing is preparing the active materials in the solution phase.[230] This can present a challenge for common conducting polymers such as PANI, PPy, and PEDOT, which are typically insoluble in most solvents.[231–233] R2R-compatible processing of these materials thus often requires surfactants to aid in solubilization.[234] Doping PANI with sulfonic acid surfactants such as dodecylbenzenesulfonic acid (DBSA) or camphorsulfonic acid (CSA), for example, greatly improves solubility,[235] allowing the effective formation of inks for gravure printing[236] or inkjet printing.[237] Doping PEDOT with PSS yields a similar effect to create homogeneous polymer suspensions and thus drastically improve processability. For applications in screen printing, the addition of PSS has the added benefit of increasing solution viscosity, making it easier to reach the $\sim 10^3$ centipoise necessary to ensure proper adhesion of screen-printing inks to their substrates.[238] It should be noted,

however, that the addition of compounds such as PSS can negatively impact the electrical conductivity of an electrode; thus, inks for spray-coating[239] or bar-coating[240] of these PEDOT:PSS solutions are often composited with carbon-based additives such as graphene to improve conductivity.

Solubilization of these materials can be achieved without the use of surfactants by functionalizing conducting polymers with solubilizing groups, further reducing the barrier to R2R-compatible synthesis. This may be accomplished through modification of the monomer – EDOT, for example, has been functionalized with alkyl chains which promote solubility in organic solvents[241,242] – or through copolymer synthesis. Österholm *et al.* demonstrated the latter approach by copolymerizing alkoxy-functionalized propylenedioxythiophene (ProDOT) units with EDOT,[243] in which the alkoxy chains of the ProDOT promoted good solubility without affecting the electrochemical performance of the PEDOT. Supercapacitor devices made from these soluble copolymers yielded energy and power densities comparable to those of electrochemically polymerized PEDOT.

In addition to the development of solution-based, R2R-compatible fabrication methods, commercialization of polymer-based supercapacitor electrodes will ultimately depend on production and material costs.[244,245] Although most conducting polymers themselves are relatively low cost – aniline in particular is cost-effective relative to the monomers of other common conducting polymers such as PPy and PEDOT[246] – it will be difficult for components such as RuO_2 to be integrated into economically-competitive devices.[247,248] In addition to eliminating these more expensive materials and minimizing the unused or wasted active material within an electrode, material costs can also be reduced by utilizing materials derived from natural sources. Several have used sodium alginate, for example, as a templating agent for conducting polymer nanofiber synthesis.[67,249] Cellulose is another popular biopolymer which can be incorporated into low-cost supercapacitor electrodes;[250–252] this material is cheap, easy to process, and naturally porous (providing a high surface area).[253,254] Cellulose-based substrates have even been made out of simple commercial printer paper.[255–257] Replacing conventional carbon materials such as CNTs or graphene with biomass-derived carbon sources presents another means of lowering the cost of hybrid supercapacitor electrodes.[17,258–260] Hu *et al.*, for example, developed a PEDOT/MnO_2 hybrid synthesized on ramie-derived carbon fibers which achieved a specific capacitance of 922 F g^{-1} at 1 A g^{-1}.[261] Finally, long-term adoption of these supercapacitor technologies will require the use of environmentally benign fabrication methods.[245] It will be necessary to adopt alternatives to the toxic or environmentally harmful reagents and solvents commonly used to process conducting polymers, including chlorinated oxidants or organic solvents such as chloroform, dichloromethane, and acetonitrile.[262]

7 Summary and outlook

Bringing conducting polymer-based supercapacitors closer to commercialization will require the fabrication of electrodes that can satisfy all of the major performance criteria addressed in this review: high specific capacitance and rate capability, high electrical conductivity, long-term cycling stability, mechanical robustness, and scalable production procedures. Depending on the intended application, however, it is often necessary to optimize for specific performance metrics, evaluating the trade-offs that exist between the various supercapacitor materials and processing techniques. In choosing a conducting polymer, for example, PANI is a particularly attractive option for most practical applications, as it has both a higher theoretical specific capacitance[53] and lower precursor cost than both PPy and PEDOT.[246] In applications requiring operation under harsh environments, however, PEDOT may be more suitable, as it has greater environmental and thermal stability.[263,264] PPy, on the other hand, has been utilized most frequently for flexible devices due to its favorable mechanical properties.[30] Furthermore, both PEDOT and PPy could be implemented in applications such as wearable electronics and bio-implantable devices, but the low biocompatibility and biodegradability of PANI would make it unsuitable for this purpose.[265] Trade-offs such as these are abundant between different polymer processing techniques as well. Solution-based synthesis methods are most scalable, for example, but often suffer from poorer performance relative to more time-intensive methods such as electropolymerization.

Our discussion herein of the fundamental processes influencing each supercapacitor performance metric and the trade-offs between them will hopefully serve as a platform for the development of next-generation polymer supercapacitors, providing insight into potential strategies for future work. Enhancing specific capacitance, one of the most important criteria in enabling supercapacitors to compete with the energy storage capabilities of batteries, will likely be accomplished through further development of nanostructures which optimize material utilization efficiency and ion accessibility. As has been the trend in recent years, we expect novel polymer–metal oxide composites to be the most effective in synergistically achieving ultrahigh capacitance levels. Optimization of specific capacitance will also be facilitated by eliminating issues with electrical conductivity in polymer-based electrodes. Efforts toward this goal should be directed towards the development of conductive binders, such that even materials prepared in powder form (*e.g.* by solution-based methods such as chemical oxidative polymerization) can be integrated into high conductivity, high performing electrodes. Further development of methods to make ultrahigh conductivity single crystal polymers, as has been done for PEDOT,[97] will also be beneficial.

Of all the performance metrics addressed in this work, long-term cycling stability is the most pressing for polymer-based electrodes. While the development of composite nanostructures to accommodate swelling and shrinking of the electrode material have shown promise thus far, more recent efforts to increase stability by enhancing the robustness of the polymer chains themselves (*e.g.* through improved molecular ordering) may prove to be even more promising in the future. Future efforts should be directed towards fundamental investigations of the effect of chain alignment, length, and defects on local strain in the polymer during cycling.

Future work will also advance the development of flexible, stretchable, or other mechanically robust polymer-based devices. Of particular interest is the development of synthetic strategies for multifunctional conducting polymers, for example by integrating both pseudocapacitive and self-healing properties into a single material. This type of approach could both simplify fabrication procedures and minimize inactive weight in a device.

Ultimately, the extent to which conducting polymer-based supercapacitors contribute to the next generation of energy storage will hinge upon their cost, which is limited by the scalability with which they are fabricated. Further efforts must be devoted to developing simple, solution-based synthesis processes which can be integrated with high-throughput R2R processing techniques without sacrificing device performance. Recent strategies to functionalize conducting polymers or create copolymers which improve solution processability while maintaining electrochemical properties are especially promising and should be investigated further.

Conflicts of interest

There are no conflicts of interest to declare.

Acknowledgements

This work was funded by the European Research Council (ERC) grant to S. K. S., EMATTER (# 280078). K. D. F. acknowledges support from the Winston Churchill Foundation of the United States. T. W. thanks the China Scholarship Council (CSC) for funding and the Engineering and Physical Sciences Research Council of the UK (EPSRC) Centre for Doctoral Training in Sensor Technologies and Applications (grant number: EP/L015889/1) for support.

References

1 International Energy Agency, *Key World Energy Statistics*, 2016.
2 A. Demirbaş, *Energy Sources, Part A*, 2006, **28**, 779–792.
3 N. L. Panwar, S. C. Kaushik and S. Kothari, *Renewable Sustainable Energy Rev.*, 2011, **15**, 1513–1524.
4 B. Dunn, H. Kamath and J.-M. Tarascon, *Science*, 2011, **334**, 928–935.
5 A. Khaligh and Z. Li, *IEEE Trans. Veh. Technol.*, 2010, **59**, 2806–2814.
6 E. Karden, S. Ploumen, B. Fricke, T. Miller and K. Snyder, *J. Power Sources*, 2007, **168**, 2–11.
7 J. R. Miller and A. F. Burke, *Electrochem. Soc. Interface*, 2008, **17**, 53–57.
8 I. Hadjipaschalis, A. Poullikkas and V. Efthimiou, *Renewable Sustainable Energy Rev.*, 2009, **13**, 1513–1522.
9 P. Simon, Y. Gogotsi and B. Dunn, *Science*, 2014, **343**, 1210–1211.
10 J. R. Miller, P. Simon and S. Patrice, *Sci. Mag.*, 2008, **321**, 651–652.
11 Y. Yao, M. T. McDowell, I. Ryu, H. Wu, N. Liu, L. Hu, W. D. Nix and Y. Cui, *Nano Lett.*, 2011, **11**, 2949–2954.
12 R. Kötz and M. Carlen, *Electrochim. Acta*, 2000, **45**, 2483–2498.
13 M. Winter and R. J. Brodd, *Chem. Rev.*, 2004, **104**, 4245–4269.
14 P. Simon and Y. Gogotsi, *Acc. Chem. Res.*, 2013, **46**, 1094–1103.
15 P. Simon and Y. Gogotsi, *Philos. Trans. R. Soc., A*, 2010, **368**, 3457–3467.
16 P. Simon and Y. Gogotsi, *Nat. Mater.*, 2008, **7**, 845–854.
17 P. J. Hall, M. Mirzaeian, S. I. Fletcher, F. B. Sillars, A. J. R. Rennie, G. O. Shitta-Bey, G. Wilson, A. Cruden and R. Carter, *Energy Environ. Sci.*, 2010, **3**, 1238–1251.
18 E. Faggioli, P. Rena, V. Danel, X. Andrieu, R. Mallant and H. Kahlen, *J. Power Sources*, 1999, **84**, 261–269.
19 W. Lhomme, P. Delarue, P. Barrade, A. Bouscayrol and A. Rufer, in *Conference Record of the 2005 Industry Applications Conference*, IEEE, 2005, vol. 1–4, pp. 2013–2020.
20 J. M. Miller and M. Everett, *Power Electron. Transp.*, 2004, 19–26.
21 E. Frackowiak and F. Béguin, *Carbon*, 2001, **39**, 937–950.
22 M. D. Stoller, S. Park, Z. Yanwu, J. An and R. S. Ruoff, *Nano Lett.*, 2008, **8**, 3498–3502.
23 A. J. Bard and L. R. Faulkner, *Electrochemical Methods: Fundamentals and Applications*, John Wiley & Sons, Inc., New York, 2nd edn, 2001, vol. 30.
24 A. G. Pandolfo and A. F. Hollenkamp, *J. Power Sources*, 2006, **157**, 11–27.
25 G. Wang, L. Zhang and J. Zhang, *Chem. Soc. Rev.*, 2012, **41**, 797–828.
26 L. L. Zhang and X. S. Zhao, *Chem. Soc. Rev.*, 2009, **38**, 2520–2531.
27 A. Borenstein, O. Hanna, R. Attias, S. Luski, T. Brousse and D. Aurbach, *J. Mater. Chem. A*, 2017, **5**, 12653–12672.
28 L. L. Zhang, R. Zhou and X. S. Zhao, *J. Mater. Chem.*, 2010, **20**, 5983–5992.
29 G. Yu, X. Xie, L. Pan, Z. Bao and Y. Cui, *Nano Energy*, 2013, **2**, 213–234.
30 I. Shown, A. Ganguly, L.-C. Chen and K.-H. Chen, *Energy Sci. Eng.*, 2015, **3**, 2–26.
31 V. Augustyn, P. Simon and B. Dunn, *Energy Environ. Sci.*, 2014, **7**, 1597–1614.
32 B. E. Conway, V. Birss and J. Wojtowicz, *J. Power Sources*, 1997, **66**, 1–14.
33 G. A. Snook, P. Kao and A. S. Best, *J. Power Sources*, 2011, **196**, 1–12.
34 Y. Zhang, H. Feng, X. Wu, L. Wang, A. Zhang, T. Xia, H. Dong, X. Li and L. Zhang, *Int. J. Hydrogen Energy*, 2009, **34**, 4889–4899.
35 Y.-Y. Peng, B. Akuzum, N. Kurra, M.-Q. Zhao, M. Alhabeb, B. Anasori, E. C. Kumbur, H. N. Alshareef, M.-D. Ger and Y. Gogotsi, *Energy Environ. Sci.*, 2016, **7**, 867–884.
36 M. Jaiswal and R. Menon, *Polym. Int.*, 2006, **55**, 1371–1384.
37 R. McNeill, R. Siudak, J. Wardlaw and D. Weiss, *Aust. J. Chem.*, 1963, **16**, 1056–1075.

38 G. Inzelt, M. Pineri, J. W. Schultze and M. A. Vorotyntsev, *Electrochim. Acta*, 2000, **45**, 2403–2421.
39 C. Yang and D. Li, *Mater. Lett.*, 2015, **155**, 78–81.
40 S. Ghosh, T. Maiyalagan and R. N. Basu, *Nanoscale*, 2016, **8**, 6921–6947.
41 L. Wang, Q. Wu, Z. Zhang, Y. Zhang, J. Pan, Y. Li, Y. Zhao, L. Zhang, X. Cheng and H. Peng, *J. Mater. Chem. A*, 2016, **4**, 3217–3222.
42 C. Choi, S. H. Kim, H. J. Sim, J. A. Lee, A. Y. Choi, Y. T. Kim, X. Lepró, G. M. Spinks, R. H. Baughman and S. J. Kim, *Sci. Rep.*, 2015, **5**, 9387.
43 J. Kim, J. Lee, J. You, M.-S. Park, M. S. Al Hossain, Y. Yamauchi and J. H. Kim, *Mater. Horiz.*, 2016, **3**, 517–535.
44 Y.-E. Miao, W. Fan, D. Chen and T. Liu, *ACS Appl. Mater. Interfaces*, 2013, **5**, 4423–4428.
45 H. Lin, L. Li, J. Ren, Z. Cai, L. Qiu, Z. Yang and H. Peng, *Sci. Rep.*, 2013, **3**, 1353.
46 A. Zucca, K. Yamagishi, T. Fujie, S. Takeoka, V. Mattoli and F. Greco, *J. Mater. Chem. C*, 2015, **3**, 6539–6548.
47 M. D. Stoller and R. S. Ruoff, *Energy Environ. Sci.*, 2010, **3**, 1294–1301.
48 C. Peng, D. Hu, G. Z. Chen, A. R. Mount, P. J. Wilson, D. Bloor, A. T. Monkman and C. M. Elliott, *Chem. Commun.*, 2011, **47**, 4105–4107.
49 A. M. Bryan, L. M. Santino, Y. Lu, S. Acharya and J. M. D'Arcy, *Chem. Mater.*, 2016, **28**, 5989–5998.
50 K. M. Molapo, P. M. Ndangili, R. F. Ajayi, G. Mbambisa, S. M. Mailu, N. Njomo, M. Masikini, P. Baker and E. I. Iwuoha, *Int. J. Electrochem. Sci.*, 2012, **7**, 11859–11875.
51 R. Pauliukaite, C. M. A. Brett and A. P. Monkman, *Electrochim. Acta*, 2004, **50**, 159–167.
52 H. Li, J. Wang, Q. Chu, Z. Wang, F. Zhang and S. Wang, *J. Power Sources*, 2009, **190**, 578–586.
53 K. Lota, V. Khomenko and E. Frackowiak, *J. Phys. Chem. Solids*, 2004, **65**, 295–301.
54 X. Ning, W. Zhong and L. Wan, *RSC Adv.*, 2016, **6**, 25519–25524.
55 H. Sheng, M. Wei, A. D'Aloia and G. Wu, *ACS Appl. Mater. Interfaces*, 2016, **8**, 30212–30224.
56 Z.-F. Li, H. Zhang, Q. Liu, L. Sun, L. Stanciu and J. Xie, *ACS Appl. Mater. Interfaces*, 2013, **5**, 2685–2691.
57 H. Kwon, D. Hong, I. Ryu and S. Yim, *ACS Appl. Mater. Interfaces*, 2017, **9**, 7412–7423.
58 Y.-Y. Horng, Y.-C. Lu, Y.-K. Hsu, C.-C. Chen, L.-C. Chen and K.-H. Chen, *J. Power Sources*, 2010, **195**, 4418–4422.
59 M. Zhang, Q. Zhou, J. Chen, X. Yu, L. Huang, Y. Li, C. Li and G. Shi, *Energy Environ. Sci.*, 2016, **9**, 2005–2010.
60 K. Wang, Q. Meng, Y. Zhang, Z. Wei and M. Miao, *Adv. Mater.*, 2013, **25**, 1494–1498.
61 S. Biswas and L. T. Drzal, *Chem. Mater.*, 2010, **22**, 5667–5671.
62 K. Wang, H. Wu, Y. Meng and Z. Wei, *Small*, 2014, **10**, 14–31.
63 J. Rodríguez-Moreno, E. Navarrete-Astorga, E. A. Dalchiele, R. Schrebler, J. R. Ramos-Barrado and F. Martín, *Chem. Commun.*, 2014, **50**, 5652–5655.
64 M. Xue, F. Li, J. Zhu, H. Song, M. Zhang and T. Cao, *Adv. Funct. Mater.*, 2012, **22**, 1284–1290.
65 B. Ma, X. Zhou, H. Bao, X. Li and G. Wang, *J. Power Sources*, 2012, **215**, 36–42.
66 S. Chaudhari, Y. Sharma, P. S. Archana, R. Jose, S. Ramakrishna, S. Mhaisalkar and M. Srinivasan, *J. Appl. Polym. Sci.*, 2013, **129**, 1660–1668.
67 Y. Li, X. Zhao, Q. Xu, Q. Zhang and D. Chen, *Langmuir*, 2011, **27**, 6458–6463.
68 Y.-Z. Long, M.-M. Li, C. Gu, M. Wan, J.-L. Duvail, Z. Liu and Z. Fan, *Prog. Polym. Sci.*, 2011, **36**, 1415–1442.
69 J. Xu, K. Wang, S.-Z. Z. Zu, B.-H. H. Han and Z. Wei, *ACS Nano*, 2010, **4**, 5019–5026.
70 P. Passiniemi, *Synth. Met.*, 1995, **69**, 685–686.
71 C. Zhou, Y. Zhang, Y. Li and J. Liu, *Nano Lett.*, 2013, **13**, 2078–2085.
72 J. Wang, Y. Xu, F. Yan, J. Zhu and J. Wang, *J. Power Sources*, 2011, **196**, 2373–2379.
73 X. Yan, Z. Tai, J. Chen and Q. Xue, *Nanoscale*, 2011, **3**, 212–216.
74 M. M. Islam, S. H. Aboutalebi, D. Cardillo, H. K. Liu, K. Konstantinov and S. X. Dou, *ACS Cent. Sci.*, 2015, **1**, 206–216.
75 J. Yan, T. Wei, B. Shao, Z. Fan, W. Qian, M. Zhang and F. Wei, *Carbon*, 2010, **48**, 487–493.
76 X. Dong, J. Wang, J. Wang, M. B. Chan-Park, X. Li, L. Wang, W. Huang and P. Chen, *Mater. Chem. Phys.*, 2012, **134**, 576–580.
77 J. Yan, T. Wei, Z. Fan, W. Qian, M. Zhang, X. Shen and F. Wei, *J. Power Sources*, 2010, **195**, 3041–3045.
78 Y. Han, M. Shen, Y. Wu, J. Zhu, B. Ding, H. Tong and X. Zhang, *Synth. Met.*, 2013, **172**, 21–27.
79 H. Zhou, W. Yao, G. Li, J. Wang and Y. Lu, *Carbon*, 2013, **59**, 495–502.
80 H. Guo, W. He, Y. Lu and X. Zhang, *Carbon*, 2015, **92**, 133–141.
81 Y. Zhao, B. Liu, L. Pan and G. Yu, *Energy Environ. Sci.*, 2013, **6**, 2856–2870.
82 L. Pan, G. Yu, D. Zhai, H. R. Lee, W. Zhao, N. Liu, H. Wang, B. C.-K. Tee, Y. Shi, Y. Cui and Z. Bao, *Proc. Natl. Acad. Sci. U. S. A.*, 2012, **109**, 9287–9292.
83 F. M. Guo, R. Q. Xu, X. Cui, L. Zhang, K. L. Wang, Y. W. Yao and J. Q. Wei, *J. Mater. Chem. A*, 2016, **4**, 9311–9318.
84 T. Raudsepp, M. Marandi, T. Tamm, V. Sammelselg and J. Tamm, *Electrochim. Acta*, 2008, **53**, 3828–3835.
85 M. D. Ingram, H. Staesche and K. S. Ryder, *J. Power Sources*, 2004, **129**, 107–112.
86 F. Shi, L. Li, X. Wang, C. Gu and J. Tu, *RSC Adv.*, 2014, **4**, 41910–41921.
87 D. F. Zeigler, S. L. Candelaria, K. A. Mazzio, T. R. Martin, E. Uchaker, S. L. Suraru, L. J. Kang, G. Cao and C. K. Luscombe, *Macromolecules*, 2015, **48**, 5196–5203.
88 Z. Wang, D. O. Carlsson, P. Tammela, K. Hua, P. Zhang, L. Nyholm and M. Strømme, *ACS Nano*, 2015, **9**, 7563–7571.
89 J. Chmiola, G. Yushin, Y. Gogotsi, C. Portet, P. Simon and P. L. Taberna, *Science*, 2006, **313**, 1760–1763.

90 S. Kondrat, C. R. Pérez, V. Presser, Y. Gogotsi and A. A. Kornyshev, *Energy Environ. Sci.*, 2012, **5**, 6474–6479.
91 J. Chmiola, G. Yushin, R. Dash and Y. Gogotsi, *J. Power Sources*, 2006, **158**, 765–772.
92 H. R. Ghenaatian, M. F. Mousavi and M. S. Rahmanifar, *Electrochim. Acta*, 2012, **78**, 212–222.
93 H. R. Ghenaatian, M. F. Mousavi, S. H. Kazemi and M. Shamsipur, *Synth. Met.*, 2009, **159**, 1717–1722.
94 W. A. Christinelli, R. Gonçalves and E. C. Pereira, *J. Power Sources*, 2016, **303**, 73–80.
95 L. Groenendaal, F. Jonas, D. Freitag, H. Pielartzik and J. R. Reynolds, *Adv. Mater.*, 2000, **12**, 481–494.
96 G. R. Mitchell, F. J. Davis and C. H. Legge, *Synth. Met.*, 1988, **26**, 247–257.
97 B. Cho, K. S. Park, J. Baek, H. S. Oh, Y. E. Koo Lee and M. M. Sung, *Nano Lett.*, 2014, **14**, 3321–3327.
98 G. Tourillon and F. Garnier, *J. Phys. Chem.*, 1983, **87**, 2289–2292.
99 W. Shi, T. Zhao, J. Xi, D. Wang and Z. Shuai, *J. Am. Chem. Soc.*, 2015, **137**, 12929–12938.
100 K. Su, N. Nuraje, L. Zhang, I.-W. Chu, R. M. Peetz, H. Matsui and N.-L. Yang, *Adv. Mater.*, 2007, **19**, 669–672.
101 O. Bubnova, Z. U. Khan, H. Wang, S. Braun, D. R. Evans, M. Fabretto, P. Hojati-Talemi, D. Dagnelund, J.-B. Arlin, Y. H. Geerts, S. Desbief, D. W. Breiby, J. W. Andreasen, R. Lazzaroni, W. M. Chen, I. Zozoulenko, M. Fahlman, P. J. Murphy, M. Berggren and X. Crispin, *Nat. Mater.*, 2013, **13**, 190–194.
102 V. Vohra and T. Anzai, *J. Nanomater.*, 2017, **2017**, 1–18.
103 D. Wu, J. Zhang, W. Dong, H. Chen, X. Huang, B. Sun and L. Chen, *Synth. Met.*, 2013, **176**, 86–91.
104 H.-P. Cong, X.-C. Ren, P. Wang and S.-H. Yu, *Energy Environ. Sci.*, 2013, **6**, 1185–1191.
105 N. A. Kumar, H. J. Choi, Y. R. Shin, D. W. Chang, L. Dai and J. B. Baek, *ACS Nano*, 2012, **6**, 1715–1723.
106 M. Kim, C. Lee and J. Jang, *Adv. Funct. Mater.*, 2014, **24**, 2489–2499.
107 H. Choi and H. Yoon, *Nanomaterials*, 2015, **5**, 906–936.
108 J. Jang, J. Bae, M. Choi and S.-H. Yoon, *Carbon*, 2005, **43**, 2730–2736.
109 J. Zhi, O. Reiser and F. Huang, *ACS Appl. Mater. Interfaces*, 2016, **8**, 8452–8459.
110 J. Luo, V. C. Tung, A. R. Koltonow, H. D. Jang and J. Huang, *J. Mater. Chem.*, 2012, **22**, 12993–12996.
111 V. C. Tung, J. Kim, L. J. Cote and J. Huang, *J. Am. Chem. Soc.*, 2011, **133**, 9262–9265.
112 M. Kang, J. E. Lee, H. W. Shim, M. S. Jeong, W. B. Im and H. Yoon, *RSC Adv.*, 2014, **4**, 27939–27945.
113 K. Shi and I. Zhitomirsky, *J. Power Sources*, 2013, **240**, 42–49.
114 C. Shi and I. Zhitomirsky, *Surf. Eng.*, 2011, **27**, 655–661.
115 S. Chen and I. Zhitomirsky, *J. Power Sources*, 2013, **243**, 865–871.
116 B. Yao, L. Huang, J. Zhang, X. Gao, J. Wu, Y. Cheng, X. Xiao, B. Wang, Y. Li and J. Zhou, *Adv. Mater.*, 2016, **28**, 6353–6358.
117 W. K. Chee, H. N. Lim, I. Harrison, K. F. Chong, Z. Zainal, C. H. Ng and N. M. Huang, *Electrochim. Acta*, 2015, **157**, 88–94.
118 C. Ma, Y. Li, J. Shi, Y. Song and L. Liu, *Chem. Eng. J.*, 2014, **249**, 216–225.
119 P. Li, Y. Yang, E. Shi, Q. Shen, Y. Shang, S. Wu, J. Wei, K. Wang, H. Zhu, Q. Yuan, A. Cao and D. Wu, *ACS Appl. Mater. Interfaces*, 2014, **6**, 5228–5234.
120 F. Xiao, S. Yang, Z. Zhang, H. Liu, J. Xiao, L. Wan, J. Luo, S. Wang and Y. Liu, *Sci. Rep.*, 2015, **5**, 9359.
121 R. Liu and B. L. Sang, *J. Am. Chem. Soc.*, 2008, **130**, 2942–2943.
122 A. Bahloul, B. Nessark, E. Briot, H. Groult, A. Mauger, K. Zaghib and C. M. Julien, *J. Power Sources*, 2013, **240**, 267–272.
123 W. Wei, X. Cui, W. Chen and D. G. Ivey, *Chem. Soc. Rev.*, 2011, **40**, 1697–1721.
124 J. Yan, Z. Fan, T. Wei, W. Qian, M. Zhang and F. Wei, *Carbon*, 2010, **48**, 3825–3833.
125 Y. Jin, H. Chen, M. Chen, N. Liu and Q. Li, *ACS Appl. Mater. Interfaces*, 2013, **5**, 3408–3416.
126 M. Zhi, A. Manivannan, F. Meng and N. Wu, *J. Power Sources*, 2012, **208**, 345–353.
127 L. Yuan, X.-H. Lu, X. Xiao, T. Zhai, J. Dai, F. Zhang, B. Hu, X. Wang, L. Gong, J. Chen, C. Hu, Y. Tong, J. Zhou and Z. L. Wang, *ACS Nano*, 2012, **6**, 656–661.
128 Q. Cheng, J. Tang, J. Ma, H. Zhang, N. Shinya and L.-C. Qin, *Carbon*, 2011, **49**, 2917–2925.
129 E. Raymundo-Piñero, V. Khomenko, E. Frackowiak and F. Béguin, *J. Electrochem. Soc.*, 2005, **152**, A229.
130 H. Jiang, J. Ma and C. Li, *Adv. Mater.*, 2012, **24**, 4197–4202.
131 J.-H. Kim, K. H. Lee, L. J. Overzet and G. S. Lee, *Nano Lett.*, 2011, **11**, 2611–2617.
132 G.-R. Li, Z.-P. Feng, Y.-N. Ou, D. Wu, R. Fu and Y.-X. Tong, *Langmuir*, 2010, **26**, 2209–2213.
133 Y. Hou, Y. Cheng, T. Hobson and J. Liu, *Nano Lett.*, 2010, **10**, 2727–2733.
134 J. Han, L. Li, P. Fang and R. Guo, *J. Phys. Chem. C*, 2012, **116**, 15900–15907.
135 R. K. Sharma, A. C. Rastogi and S. B. Desu, *Electrochim. Acta*, 2008, **53**, 7690–7695.
136 G. Yu, L. Hu, N. Liu, H. Wang, M. Vosgueritchian, Y. Yang, Y. Cui and Z. Bao, *Nano Lett.*, 2011, **11**, 4438–4442.
137 T. Qian, N. Xu, J. Zhou, T. Yang, X. Liu, X. Shen, J. Liang and C. Yan, *J. Mater. Chem. A*, 2015, **3**, 488–493.
138 W. Xiong, X. Hu, X. Wu, Y. Zeng, B. Wang, G. He and Z. Zhu, *J. Mater. Chem. A*, 2015, **3**, 17209–17216.
139 L. Wang, X. Feng, L. Ren, Q. Piao, J. Zhong, Y. Wang, H. Li, Y. Chen and B. Wang, *J. Am. Chem. Soc.*, 2015, **137**, 4920–4923.
140 D. Fu, H. Li, X.-M. Zhang, G. Han, H. Zhou and Y. Chang, *Mater. Chem. Phys.*, 2016, **179**, 166–173.
141 D. Sheberla, J. C. Bachman, J. S. Elias, C. J. Sun, Y. Shao-Horn and M. Dincă, *Nat. Mater.*, 2017, **16**, 220–224.
142 T. Wang, M. Farajollahi, S. Henke, T. Zhu, S. R. Bajpe, S. Sun, J. S. Barnard, J. S. Lee, J. D. W. Madden, A. K. Cheetham and S. K. Smoukov, *Mater. Horiz.*, 2017, **4**, 64–71.
143 T. Brousse, P.-L. Taberna, O. Crosnier, R. Dugas, P. Guillemet, Y. Scudeller, Y. Zhou, F. Favier, D. Bélanger and P. Simon, *J. Power Sources*, 2007, **173**, 633–641.

144 Y. Song, T.-Y. Liu, X.-X. Xu, D.-Y. Feng, Y. Li and X.-X. Liu, *Adv. Funct. Mater.*, 2015, **25**, 4626–4632.
145 T. Liu, L. Finn, M. Yu, H. Wang, T. Zhai, X. Lu, Y. Tong and Y. Li, *Nano Lett.*, 2014, **14**, 2522–2527.
146 R. Ranjusha, K. M. Sajesh, S. Roshny, V. Lakshmi, P. Anjali, T. S. Sonia, A. Sreekumaran Nair, K. R. V. Subramanian, S. V. Nair, K. P. Chennazhi and A. Balakrishnan, *Microporous Mesoporous Mater.*, 2014, **186**, 30–36.
147 H. Yin, S. Zhao, J. Wan, H. Tang, L. Chang, L. He, H. Zhao, Y. Gao and Z. Tang, *Adv. Mater.*, 2013, **25**, 6270–6276.
148 C. Peng, S. Zhang, D. Jewell and G. Z. Chen, *Prog. Nat. Sci.*, 2008, **18**, 777–788.
149 G.-P. Hao, F. Hippauf, M. Oschatz, F. M. Wisser, A. Leifert, W. Nickel, N. Mohamed-Noriega, Z. Zheng and S. Kaskel, *ACS Nano*, 2014, **8**, 7138–7146.
150 W. Zhao, S. Wang, C. Wang, S. Wu, W. Xu, M. Zou, A. Ouyang, A. Cao and Y. Li, *Nanoscale*, 2016, **8**, 626–633.
151 W. Zhao, Y. Li, S. Wu, D. Wang, X. Zhao, F. Xu, M. Zou, H. Zhang, X. He and A. Cao, *ACS Appl. Mater. Interfaces*, 2016, **8**, 34027–34033.
152 R. Malik, L. Zhang, C. McConnell, M. Schott, Y.-Y. Hsieh, R. Noga, N. T. Alvarez and V. Shanov, *Carbon*, 2017, **116**, 579–590.
153 G. Wu, P. Tan, D. Wang, Z. Li, L. Peng, Y. Hu, C. Wang, W. Zhu, S. Chen and W. Chen, *Sci. Rep.*, 2017, **7**, 43676.
154 Y. Chen, L. Du, P. Yang, P. Sun, X. Yu and W. Mai, *J. Power Sources*, 2015, **287**, 68–74.
155 R. R. Salunkhe, S.-H. Hsu, K. C. W. Wu and Y. Yamauchi, *ChemSusChem*, 2014, **7**, 1551–1556.
156 J. Zhang and X. S. Zhao, *J. Phys. Chem. C*, 2012, **116**, 5420–5426.
157 K. Li, J. Liu, Y. Huang, F. Bu and Y. Xu, *J. Mater. Chem. A*, 2017, **5**, 5466–5474.
158 M. Zhu, Y. Huang, Q. Deng, J. Zhou, Z. Pei, Q. Xue, Y. Huang, Z. Wang, H. Li, Q. Huang and C. Zhi, *Adv. Energy Mater.*, 2016, **6**, 1600969.
159 M. Boota, B. Anasori, C. Voigt, M. Q. Zhao, M. W. Barsoum and Y. Gogotsi, *Adv. Mater.*, 2016, **28**, 1517–1522.
160 J. Luo, W. Zhong, Y. Zou, C. Xiong and W. Yang, *J. Power Sources*, 2016, **319**, 73–81.
161 W. Li, H. Lu, N. Zhang and M. Ma, *ACS Appl. Mater. Interfaces*, 2017, **9**, 20142–20149.
162 W. Li, F. Gao, X. Wang, N. Zhang and M. Ma, *Angew. Chem., Int. Ed.*, 2016, **55**, 9196–9201.
163 K. D. Fong, T. Wang, H.-K. Kim, R. V. Kumar and S. K. Smoukov, *ACS Energy Lett.*, 2017, **2**, 2014–2020.
164 Y. Huang, M. Zhu, Z. Pei, Y. Huang, H. Geng and C. Zhi, *ACS Appl. Mater. Interfaces*, 2016, **8**, 2435–2440.
165 W. Tian, X. Mao, P. Brown, G. C. Rutledge and T. A. Hatton, *Adv. Funct. Mater.*, 2015, **25**, 4803–4813.
166 R. Wang, Q. Wu, X. Zhang, Z. Yang, L. Gao, J. Ni and O. K. C. Tsui, *J. Mater. Chem. A*, 2016, **4**, 12602–12608.
167 C. Xia, W. Chen, X. Wang, M. N. Hedhili, N. Wei and H. N. Alshareef, *Adv. Energy Mater.*, 2015, **5**, 1401805.
168 M. Shao, Z. Li, R. Zhang, F. Ning, M. Wei, D. G. Evans and X. Duan, *Small*, 2015, **11**, 3530–3538.
169 H. Wei, Y. Wang, J. Guo, X. Yan, R. O'Connor, X. Zhang, N. Z. Shen, B. L. Weeks, X. Huang, S. Wei and Z. Guo, *ChemElectroChem*, 2015, **2**, 119–126.
170 H. Yang, Y. Y. Liu, Z. Wang, Y. Y. Liu, H. Du and X. Hao, *J. Appl. Polym. Sci.*, 2016, **133**, 43418.
171 E. Frackowiak, V. Khomenko, K. Jurewicz, K. Lota and F. Béguin, *J. Power Sources*, 2006, **153**, 413–418.
172 M. Gao, G. Zhang, G. Zhang, X. Wang, S. Wang and Y. Yang, *Polym. Degrad. Stab.*, 2011, **96**, 1799–1804.
173 L. D. Arsov, W. Plieth and G. Koßmehl, *J. Solid State Electrochem.*, 1998, **2**, 355–361.
174 P. Tehrani, A. Kanciurzewska, X. Crispin, N. D. Robinson, M. Fahlman and M. Berggren, *Solid State Ionics*, 2007, **177**, 3521–3527.
175 U. Barsch and F. Beck, *Electrochim. Acta*, 1996, **41**, 1761–1771.
176 A. J. Oostra, K. H. W. van den Bos, P. W. M. Blom and J. J. Michels, *J. Phys. Chem. B*, 2013, **117**, 10929–10935.
177 Z. Dai, C. Peng, J. H. Chae, K. C. Ng and G. Z. Chen, *Sci. Rep.*, 2015, **5**, 9854.
178 L. M. Santino, S. Acharya and J. M. D'Arcy, *J. Mater. Chem. A*, 2017, **5**, 11772–11780.
179 N. Choudhary, C. Li, J. Moore, N. Nagaiah, L. Zhai, Y. Jung and J. Thomas, *Adv. Mater.*, 2017, **29**, 1605336.
180 C. Zhong, Y. Deng, W. Hu, J. Qiao, L. Zhang and J. Zhang, *Chem. Soc. Rev.*, 2015, **44**, 7484–7539.
181 L. M. Santino, Y. Lu, S. Acharya, L. Bloom, D. Cotton, A. Wayne and J. M. D'Arcy, *ACS Appl. Mater. Interfaces*, 2016, **8**, 29452–29460.
182 M. F. El-Kady, V. Strong, S. Dubin and R. B. Kaner, *Science*, 2012, **335**, 1326–1330.
183 M. Kaempgen, C. K. Chan, J. Ma, Y. Cui and G. Gruner, *Nano Lett.*, 2009, **9**, 1872–1876.
184 D.-W. Wang, F. Li, J. Zhao, W. Ren, Z.-G. Chen, J. Tan, Z.-S. Wu, I. Gentle, G. Q. Lu and H.-M. Cheng, *ACS Nano*, 2009, **3**, 1745–1752.
185 C. Meng, C. Liu, L. Chen, C. Hu and S. Fan, *Nano Lett.*, 2010, **10**, 4025–4031.
186 X. Zhao, M. Dong, J. Zhang, Y. Li and Q. Zhang, *Nanotechnology*, 2016, **27**, 385705.
187 Y. Zhou, X. Hu, Y. Shang, C. Hua, P. Song, X. Li, Y. Zhang and A. Cao, *RSC Adv.*, 2016, **6**, 62062–62070.
188 F. Meng and Y. Ding, *Adv. Mater.*, 2011, **23**, 4098–4102.
189 C. Zhang, T. M. Higgins, S.-H. Park, S. E. O'Brien, D. Long, J. N. Coleman and V. Nicolosi, *Nano Energy*, 2016, **28**, 495–505.
190 K. Wang, X. Zhang, X. Sun and Y. Ma, *Sci. China Mater.*, 2016, **59**, 412–420.
191 Y. Shi, L. Pan, B. Liu, Y. Wang, Y. Cui, Z. Bao, G. Yu, Y. X. Tong, Y. Li, T. Yu, H. J. Fan, E. M. Benito, F. J. Touwslager, A. W. Marsman, B. J. E. Van Rens and D. M. De Leeuw, *J. Mater. Chem. A*, 2014, **2**, 6086–6091.
192 Y. Huang, M. Zhong, Y. Huang, M. Zhu, Z. Pei, Z. Wang, Q. Xue, X. Xie and C. Zhi, *Nat. Commun.*, 2015, **6**, 10310.
193 Z. Zhang, J. Deng, X. Li, Z. Yang, S. He, X. Chen, G. Guan, J. Ren and H. Peng, *Adv. Mater.*, 2015, **27**, 356–362.

194 Y. Huang, Y. Huang, M. Zhu, W. Meng, Z. Pei, C. Liu, H. Hu and C. Zhi, *ACS Nano*, 2015, **9**, 6242–6251.
195 Z. Niu, W. Zhou, X. Chen, J. Chen and S. Xie, *Adv. Mater.*, 2015, **27**, 6002–6008.
196 C. Yan and P. S. Lee, *Small*, 2014, **10**, 3443–3460.
197 J. A. Rogers, T. Someya and Y. Huang, *Science*, 2010, **327**, 1603–1607.
198 N. Lu and D.-H. Kim, *Soft Robotics*, 2014, **1**, 53–62.
199 J. S. Noh, *Polymers*, 2016, **8**, 123.
200 B. Yue, C. Wang, X. Ding and G. G. Wallace, *Electrochim. Acta*, 2012, **68**, 18–24.
201 J. Yu, W. Lu, S. Pei, K. Gong, L. Wang, L. Meng, Y. Huang, J. P. Smith, K. S. Booksh, Q. Li, J. H. Byun, Y. Oh, Y. Yan and T. W. Chou, *ACS Nano*, 2016, **10**, 5204–5211.
202 T. Chen, H. Peng, M. Durstock and L. Dai, *Sci. Rep.*, 2014, **4**, 3612.
203 N. Zhang, W. Zhou, Q. Zhang, P. Luan, L. Cai, F. Yang, X. Zhang, Q. Fan, W. Zhou, Z. Xiao, X. Gu, H. Chen, K. Li, S. Xiao, Y. Wang, H. Liu and S. Xie, *Nanoscale*, 2015, **7**, 12492–12497.
204 H. Wang, B. Zhu, W. Jiang, Y. Yang, W. R. Leow, H. Wang and X. Chen, *Adv. Mater.*, 2014, **26**, 3638–3643.
205 T. Wu and B. Chen, *ACS Appl. Mater. Interfaces*, 2016, **8**, 24071–24078.
206 Y. Yang and M. W. Urban, *Chem. Soc. Rev.*, 2013, **42**, 7446.
207 M. D. Hager, P. Greil, C. Leyens, S. Van Der Zwaag and U. S. Schubert, *Adv. Mater.*, 2010, **22**, 5424–5430.
208 P. Cordier, F. Tournilhac, C. Soulié-Ziakovic and L. Leibler, *Nature*, 2008, **451**, 977–980.
209 H. Sun, X. You, Y. Jiang, G. Guan, X. Fang, J. Deng, P. Chen, Y. Luo and H. Peng, *Angew. Chem.*, 2014, **126**, 9680–9685.
210 S. Wang, N. Liu, J. Su, L. Li, F. Long, Z. Zou, X. Jiang and Y. Gao, *ACS Nano*, 2017, **11**, 2066–2074.
211 T. J. Trivedi, D. Bhattacharjya, J.-S. Yu and A. Kumar, *ChemSusChem*, 2015, **8**, 3294–3303.
212 Y. Guo, X. Zhou, Q. Tang, H. Bao, G. Wang and P. Saha, *J. Mater. Chem. A*, 2016, **4**, 8769–8776.
213 X. Liu, D. Wu, H. Wang and Q. Wang, *Adv. Mater.*, 2014, **26**, 4370–4375.
214 F. Tao, L. Qin, Z. Wang and Q. Pan, *ACS Appl. Mater. Interfaces*, 2017, **9**, 15541–15548.
215 Y. Shi, M. Wang, C. Ma, Y. Wang, X. Li and G. Yu, *Nano Lett.*, 2015, **15**, 6276–6281.
216 J. Hur, K. Im, S. W. Kim, J. Kim, D.-Y. Chung, T.-H. Kim, K. H. Jo, J. H. Hahn, Z. Bao, S. Hwang and N. Park, *ACS Nano*, 2014, **8**, 10066–10076.
217 J. Y. Oh, S. Kim, H.-K. Baik and U. Jeong, *Adv. Mater.*, 2016, **28**, 4455–4461.
218 G. Nyström, A. Marais, E. Karabulut, L. Wågberg, Y. Cui and M. M. Hamedi, *Nat. Commun.*, 2015, **6**, 7259.
219 C. Das, S. Chatterjee, G. Kumaraswamy and K. Krishnamoorthy, *J. Phys. Chem. C*, 2017, **121**, 3270–3278.
220 Q. Wu, J. Wei, B. Xu, X. Liu, H. Wang, W. Wang, Q. Wang and W. Liu, *Sci. Rep.*, 2017, **7**, 41566.
221 Y. Zhao, J. Liu, Y. Hu, H. Cheng, C. Hu, C. Jiang, L. Jiang, A. Cao and L. Qu, *Adv. Mater.*, 2013, **25**, 591–595.
222 S. Lyu, H. Chang, F. Fu, L. Hu, J. Huang and S. Wang, *J. Power Sources*, 2016, **327**, 438–446.
223 P. Andersson, R. Forchheimer, P. Tehrani and M. Berggren, *Adv. Funct. Mater.*, 2007, **17**, 3074–3082.
224 A. Hübler, B. Trnovec, T. Zillger, M. Ali, N. Wetzold, M. Mingebach, A. Wagenpfahl, C. Deibel and V. Dyakonov, *Adv. Energy Mater.*, 2011, **1**, 1018–1022.
225 P. Kopola, M. Tuomikoski, R. Suhonen and A. Maaninen, *Thin Solid Films*, 2009, **517**, 5757–5762.
226 P. Kovacik, G. del Hierro, W. Livernois and K. K. Gleason, *Mater. Horiz.*, 2015, **2**, 221–227.
227 T. Wang, M. Farajollahi, Y. S. Choi, I.-T. Lin, J. E. Marshall, N. M. Thompson, S. Kar-Narayan, J. D. W. Madden and S. K. Smoukov, *Interface Focus*, 2016, **6**, 20160026.
228 Z. Wang, P. Tammela, J. Huo, P. Zhang, M. Strømme and L. Nyholm, *J. Mater. Chem. A*, 2016, **4**, 1714–1722.
229 Y. Shi, L. Peng, Y. Ding, Y. Zhao and G. Yu, *Chem. Soc. Rev.*, 2015, **44**, 6684–6696.
230 R. R. Søndergaard, M. Hösel and F. C. Krebs, *J. Polym. Sci., Part B: Polym. Phys.*, 2013, **51**, 16–34.
231 J. F. Ponder, A. M. Österholm and J. R. Reynolds, *Macromolecules*, 2016, **49**, 2106–2111.
232 A. Kausaite-Minkstimiene, V. Mazeiko, A. Ramanaviciene and A. Ramanavicius, *Colloids Surf., A*, 2015, **483**, 224–231.
233 Z. Qiang, G. Liang, A. Gu and L. Yuan, *Mater. Lett.*, 2014, **115**, 159–161.
234 Y. Xu, I. Hennig, D. Freyberg, A. James Strudwick, M. Georg Schwab, T. Weitz and K. Chih-Pei Cha, *J. Power Sources*, 2014, **248**, 483–488.
235 M. J. R. Cardoso, M. F. S. Lima and D. M. Lenz, *Mater. Res.*, 2007, **10**, 425–429.
236 T. Mäkelä, T. Haatainen, P. Majander and J. Ahopelto, *Microelectron. Eng.*, 2007, **84**, 877–879.
237 K. Crowley, E. O'Malley, A. Morrin, M. R. Smyth and A. J. Killard, *Analyst*, 2008, **133**, 391–399.
238 S. Cho, M. Kim and J. Jang, *ACS Appl. Mater. Interfaces*, 2015, **7**, 10213–10227.
239 Z. Liu, Z.-S. Wu, S. Yang, R. Dong, X. Feng and K. Müllen, *Adv. Mater.*, 2016, **28**, 2217–2222.
240 Y. Liu, B. Weng, J. M. Razal, Q. Xu, C. Zhao, Y. Hou, S. Seyedin, R. Jalili, G. G. Wallace and J. Chen, *Sci. Rep.*, 2015, **5**, 17045.
241 A. Kumar and J. R. Reynolds, *Macromolecules*, 1996, **29**, 7629–7630.
242 B. Sankaran and J. R. Reynolds, *Macromolecules*, 1997, **30**, 2582–2588.
243 A. M. Österholm, J. F. Ponder, J. A. Kerszulis and J. R. Reynolds, *ACS Appl. Mater. Interfaces*, 2016, **8**, 13492–13498.
244 R. B. Betrián, *Boletín del Grup. Español del Carbón*, 2015, vol. 37, pp. 9–13.
245 B. Dyatkin, V. Presser, M. Heon, M. R. Lukatskaya, M. Beidaghi and Y. Gogotsi, *ChemSusChem*, 2013, **6**, 2269–2280.
246 S. Chabi, C. Peng, D. Hu and Y. Zhu, *Adv. Mater.*, 2014, **26**, 2440–2445.

247 T.-Y. Wei, C.-H. Chen, H.-C. Chien, S.-Y. Lu and C.-C. Hu, *Adv. Mater.*, 2010, **22**, 347–351.
248 C. Fu and P. S. Grant, *ACS Sustainable Chem. Eng.*, 2015, **3**, 2831–2838.
249 Y. Yu, S. Zhihuai, S. Chen, C. Bian, A. Wei Chen and G. Xue, *Langmuir*, 2006, **22**, 3899–3905.
250 X. Wang, K. Gao, Z. Shao, X. Peng, X. Wu and F. Wang, *J. Power Sources*, 2014, **249**, 148–155.
251 B. Anothumakkool, R. Soni, S. N. Bhange and S. Kurungot, *Energy Environ. Sci.*, 2015, **8**, 1339–1347.
252 H. Wang, L. Bian, P. Zhou, J. Tang and W. Tang, *J. Mater. Chem. A*, 2013, **1**, 578–584.
253 C. Liu, E. I. Gillette, X. Chen, A. J. Pearse, A. C. Kozen, M. A. Schroeder, K. E. Gregorczyk, S. B. Lee and G. W. Rubloff, *Nat. Nanotechnol.*, 2014, **9**, 1031–1039.
254 Z. Weng, Y. Su, D. W. Wang, F. Li, J. Du and H. M. Cheng, *Adv. Energy Mater.*, 2011, **1**, 917–922.
255 L. Yuan, B. Yao, B. Hu, K. Huo, W. Chen and J. Zhou, *Energy Environ. Sci.*, 2013, **6**, 470–476.
256 B. Yao, J. Zhang, T. Kou, Y. Song, T. Liu and Y. Li, *Adv. Sci.*, 2017, **4**, 1700107.
257 B. Yao, L. Yuan, X. Xiao, J. Zhang, Y. Qi, J. Zhou, J. Zhou, B. Hu and W. Chen, *Nano Energy*, 2013, **2**, 1071–1078.
258 Z. Ling, Z. Wang, M. Zhang, C. Yu, G. Wang, Y. Dong, S. Liu, Y. Wang and J. Qiu, *Adv. Funct. Mater.*, 2016, **26**, 111–119.
259 X. L. Wu, T. Wen, H. L. Guo, S. Yang, X. Wang and A. W. Xu, *ACS Nano*, 2013, **7**, 3589–3597.
260 Y. Ren, Q. Xu, J. Zhang, H. Yang, B. Wang, D. Yang, J. Hu and Z. Liu, *ACS Appl. Mater. Interfaces*, 2014, **6**, 9689–9697.
261 X. Hu, W. Xiong, W. Wang, S. Qin, H. Cheng, Y. Zeng, B. Wang and Z. Zhu, *ACS Sustainable Chem. Eng.*, 2016, **4**, 1201–1211.
262 F. P. Byrne, S. Jin, G. Paggiola, T. H. M. Petchey, J. H. Clark, T. J. Farmer, A. J. Hunt, C. Robert McElroy and J. Sherwood, *Sustainable Chem. Processes*, 2016, **4**, 1–24.
263 F. Vidal, C. Plesse, P. H. Aubert, L. Beouch, F. Tran-Van, G. Palaprat, P. Verge, P. Yammine, J. Citerin, A. Kheddar, L. Sauques, C. Chevrota and D. Teyssié, *Polym. Int.*, 2010, **59**, 313–320.
264 D. D. Zhou, X. T. Cui, A. Hines and R. J. Greenberg, in *Implantable Neural Prostheses 2*, Springer, New York, 2010, pp. 217–252.
265 R. Balint, N. J. Cassidy and S. H. Cartmell, *Acta Biomater.*, 2014, **10**, 2341–2353.